JOURNAL OF VIROLOGY, Sept. 2010, p. 9516–9532 Vol. 84, No. 18
0022-538X/10/$12.00 doi:10.1128/JVI.00775-10

A Short N-Terminal Peptide Motif on Flavivirus Nonstructural Protein NS1 Modulates Cellular Targeting and Immune Recognition▽

Soonjeon Youn,[1] Hyelim Cho,[2] Daved H. Fremont,[3,4,5] and Michael S. Diamond[1,2,3,5]*

Departments of Medicine,[1] Molecular Microbiology,[2] Pathology and Immunology,[3] and Biochemistry and Molecular Biophysics,[4] and the Midwest Regional Center of Excellence for Biodefense and Emerging Infectious Diseases Research,[5] Washington University School of Medicine, Saint Louis, Missouri 63110

Received 12 April 2010/Accepted 21 June 2010

Flavivirus NS1 is a versatile nonstructural glycoprotein, with intracellular NS1 functioning as an essential cofactor for viral replication and cell surface and secreted NS1 antagonizing complement activation. Even though NS1 has multiple functions that contribute to virulence, the genetic determinants that regulate the spatial distribution of NS1 in cells among different flaviviruses remain uncharacterized. Here, by creating a panel of West Nile virus-dengue virus (WNV-DENV) NS1 chimeras and site-specific mutants, we identified a novel, short peptide motif immediately C-terminal to the signal sequence cleavage position that regulates its transit time through the endoplasmic reticulum and differentially directs NS1 for secretion or plasma membrane expression. Exchange of two amino acids within this motif reciprocally changed the cellular targeting pattern of DENV or WNV NS1. For WNV, this substitution also modulated infectivity and antibody-induced phagocytosis of infected cells. Analysis of a mutant lacking all three conserved N-linked glycosylation sites revealed an independent requirement of N-linked glycans for secretion but not for plasma membrane expression of WNV NS1. Collectively, our experiments define the requirements for cellular targeting of NS1, with implications for the protective host responses, immune antagonism, and association with the host cell sorting machinery. These studies also suggest a link between the effects of NS1 on viral replication and the levels of secreted or cell surface NS1.

West Nile virus (WNV) is a single-stranded, positive-sense enveloped RNA *Flavivirus* that cycles in nature between birds and *Culex* mosquitoes. It is endemic in parts of Africa, Europe, the Middle East, and Asia, and outbreaks occur annually in North America. More than 29,000 human cases of severe WNV infection have been diagnosed in the United States since its entry in 1999, and millions have been infected and remain undiagnosed (9). Humans can develop a febrile illness that progresses to a flaccid paralysis, meningitis, or encephalitis syndrome (59). Dengue virus (DENV) is a genetically related flavivirus that is transmitted by *Aedes aegypti* and *Aedes albopictus* mosquitoes and causes clinical syndromes in humans, ranging from an acute self-limited febrile illness (dengue fever [DF]) to a severe and life-threatening vascular leakage and bleeding diathesis (dengue hemorrhagic fever/dengue shock syndrome [DHF/DSS]). Globally, DENV causes an estimated 50 million infections annually, resulting in 500,000 hospitalizations and ~22,000 deaths (45).

The ~10.7-kb *Flavivirus* RNA genome is translated as a single polyprotein, which is then cleaved into three structural proteins (C, prM/M, and E) and seven nonstructural (NS) proteins (NS1, NS2A, NS2B, NS3, NS4A, NS4B, and NS5) by virus- and host-encoded proteases (39). The multifunctional NS proteins include an RNA-dependent RNA polymerase and methyltransferase (NS5), a helicase and protease (NS3), accessory proteins that form part of the viral replication complex, and immune evasion molecules (33, 34). Flavivirus NS1 is a 48-kDa nonstructural glycoprotein with two or three N-linked glycans, depending on the flavivirus, and is absent from the virion. The Japanese encephalitis virus (JEV) serogroup (West Nile, Japanese, Murray Valley, and St. Louis encephalitis viruses) generate NS1 and NS1′ proteins, the latter of which is a product of a ribosomal frameshift event that occurs at a heptanucleotide motif located at the beginning of the NS2A gene (25, 47).

NS1 is an essential gene as it is required for efficient viral RNA replication (34, 41, 44). In infected mammalian cells, NS1 is synthesized as a soluble monomer, dimerizes after posttranslational modification in the lumen of the endoplasmic reticulum (ER), and accumulates extracellularly as higher-order oligomers, including hexamers (16, 26, 64, 65). Soluble NS1 binds back to the plasma membrane of uninfected cells through interactions with sulfated glycosaminoglycans (5). In infected cells, NS1 is also directly transported to and expressed on the plasma membrane although it lacks a transmembrane domain or canonical targeting motif. The mechanism of cell surface expression of flavivirus NS1 in infected cells remains uncertain although some fraction may be linked through an atypical glycosyl-phosphatidylinositol anchor (30, 50) or lipid rafts (49).

NS1 has been implicated in having pathogenic consequences in flavivirus infection. The high levels of NS1 in the serum of DENV-infected patients correlate with severe disease (4, 37). NS1 has been proposed to facilitate immune complex formation (4), elicit auto-antibodies that react with host matrix proteins (21), damage endothelial cells via antibody-dependent complement-mediated cytolysis (38), or directly enhance infec-

* Corresponding author. Mailing address: Departments of Medicine, Molecular Microbiology, and Pathology and Immunology, Washington University School of Medicine, 660 South Euclid Ave., Box 8051, Saint Louis, MO 63110. Phone: (314) 362-2842. Fax: (314) 362-9230. E-mail: diamond@borcim.wustl.edu.

▽ Published ahead of print on 30 June 2010.

tion (1). Flavivirus NS1 also has direct immune evasion functions and antagonizes complement activation on cell surfaces and in solution. WNV NS1 attenuates the alternative pathway of complement activation by binding the complement-regulatory protein factor H (11, 36), and DENV, WNV, and YFV NS1 proteins bind C1s and C4 in a complex to promote efficient degradation of C4 to C4b (3).

Although NS1 is absent from the virion, antibodies against it can protect against infection *in vivo*. Immunization with purified NS1 or passive administration of some anti-WNV, anti-yellow fever virus (YFV), and anti-DENV NS1 monoclonal antibodies (MAbs) protect mice against lethal virus challenge (12, 13, 17, 22, 27, 29, 31, 32, 56–58). Initial studies with isotype switch variants and $F(ab')_2$ fragments of anti-YFV NS1 MAbs suggested that the Fc region of anti-NS1 MAbs was required for protection (58). Subsequent mechanistic studies with WNV NS1 indicated that only MAbs recognizing cell surface-associated NS1 trigger Fc-γ receptor I- and/or IV-mediated phagocytosis and clearance of infected cells (13).

In this study, we identify a reciprocal relationship between the secretion and cell surface expression patterns of WNV and DENV NS1s. Using WNV-DENV NS1 chimeras and point mutants, we identified a novel short peptide motif immediately C-terminal to the signal sequence cleavage position that directs NS1 for secretion or to the plasma membrane. These studies begin to explain how NS1 regulates its localization to several cellular compartments (ER, cell surface, and extracellular space) and have implications for viral infectivity, association with the host cell sorting machinery, and protective immune responses.

MATERIALS AND METHODS

Cells and viruses. BHK21 (clone 15) cells were grown in Dulbecco's modified Eagle's medium (DMEM) supplemented with 10% fetal bovine serum (FBS), penicillin, streptomycin, 10 mM HEPES, pH 7.3, and nonessential amino acids in a 5% humidified CO_2 incubator at 37°C. C6/36 *A. albopictus* mosquito cells were grown in Leibovitz-15 medium containing 10% FBS and 10 mM HEPES at 25°C. Experiments were performed with the New York 1999 and 2000 strains of WNV (20) and the 16681 and New Guinea C strains of DENV type 2 (DENV-2) (28). Stocks of these viruses were generated in C6/36 cells, and titers were determined by plaque assay on BHK21 cells.

Generation of wild-type and chimeric NS1s. DENV NS1 (nucleotides 2353 to 3477) was amplified by PCR from an infectious cDNA clone of DENV-2(pD2/IC; strain 16681) (35) using the following primers (NS1 sequences underlined): forward, 5′-GCGGCCGCACCATGGTCTCACTGTCTGTGACACTAG-3′; reverse, 5′-TCAAGCTGTGACCAAGGAGTTGAC-3′. Alternatively, DENV-2 NS1 (New Guinea C strain) was reverse transcribed and amplified by PCR from viral RNA harvested from infected BHK21 cells using the following primers: forward, 5′-GCGGCCGCGCCACCATGGCCTCACTGTCTGTGTCACTAG-3′; reverse, 5′-GCGGCCGCTTAGGCTGTGACCAAGGAGTTGAC-3′. WNV NS1 (nucleotides 2398 to 3525) was reverse transcribed and amplified by PCR from viral RNA obtained from WNV strain New York 1999 using the following primers: forward, 5′-GTGGATGGGCGGCCGCACCATGGATAGGTCCATAGCTCTCACG-3′; reverse, 5′-CATTGACTGCGGCCGCTAAGCATTCACTTGTGACTGCAC-3′. Amplified DENV and WNV NS1 also contain 24 and 25 additional amino acids, respectively, from the C terminus of the E protein, which serve as natural leader sequences. NS1 cDNAs were subcloned into the pSTBlue TA cloning vector (Novagen). By convention, chimeras were named with the first letter referring to N-terminal portion of the flavivirus NS1 (D, DENV; W, WNV), followed by the amino acid number used for ligation to the C-terminal portion of the heterologous NS1.

DENV and WNV NS1 chimeras D269W and W269D were constructed using conserved NcoI restriction enzyme recognition sites. pSTBlue plasmids containing DENV or WNV NS1 were digested with NcoI and XhoI. The clone containing DENV NS1 nucleotides 1 to 887 and WNV NS1 nucleotides 888 to 1128 was named as D269W, with the reciprocal clone was named W269D. W158D and D158W were constructed after a silent EcoRI restriction site was introduced in WNV NS1 by changing AG to TG at nucleotides 526 and 527 using QuikChange II Site-Directed Mutagenesis Kits (Stratagene, La Jolla, CA). DENV and WNV NS1 plasmids, the latter with the newly introduced EcoRI site, were digested with EcoRI. The N-terminal fragment of DENV NS1 was ligated to the C-terminal fragment of WNV NS1 to generate D158W, and the reciprocal ligation was performed to produce W158D.

An additional series of WNV and DENV NS1 chimeras was constructed targeting sites where more than 4 amino acids are conserved in NS1 proteins of the two viruses. These DENV-WNV chimeras were constructed using a "No see'm" cloning strategy (67) using the type II restriction enzyme BsmBI (Fermentas). This enzyme recognizes a specific (5′-CGTCTCNNNNNN-3′) sequence, but cleavage leaves a 1-nucleotide 3′ overhang and 5-nucleotide 5′ overhang that are nonpalindromic. This property allows introduction of BsmBI restriction enzyme sites near the target sequence; upon ligation, the restriction enzyme sites disappear, resulting in no nucleotide sequence change. BsmBI restriction enzyme recognition sequences were introduced with QuikChange II mutagenesis. For construction of A5V/I6V (AI5VV), IS8WK, RQ10NK, R10N, or Q11K single or double point mutations, substitutions were introduced to pSTBlue WNV NS1 with a QuikChange II Site-Directed Mutagenesis Kit. Similarly, NK10RQ variants in DENV-2 (strain New Guinea C) were generated by QuikChange II site-directed mutagenesis. All oligonucleotide primers used in mutagenesis or chimerization of NS1 are available upon request.

Generation of recombinant SINVs expressing wild-type and chimeric NS1. Recombinant wild-type or chimeric NS1 was expressed transgenically using a double subgenomic Sindbis virus (SINV) expression system. Recombinant SINVs were constructed using the infectious clone p39-E2H55K70 (p39HK; gift of W. Klimstra, Pittsburgh, PA) as described previously (55). The wild-type or chimeric NS1 gene was digested with NotI from the pSTBlue vector. The p39HK SINV vector was linearized with NotI, dephosphorylated with calf intestine phosphatase (Promega), and ligated with gel-purified digested NS1. Recombinant SINV encoding the NS1 gene (SINV-NS1) was produced after *in vitro* transcription of XhoI-digested, linearized plasmids using SP6 polymerase (mMESSAGE-mMACHINE SP6 kit; Ambion) for 2 h at 37°C. After *in vitro* transcription, RNA was electroporated into BHK21 cells using a GenePulser Xcell electroporator (Bio-Rad) at 850 V and 25 μF with infinite Ω. A passage 0 (P-0) stock of recombinant SINV was harvested within 48 h, a time when 90% of cells showed cytopathic effect. Titers of recombinant viruses were determined by plaque assay on BHK21 cells, and, unless otherwise noted, all experiments were performed with the P-0 stock.

Generation of recombinant WNVs. Recombinant WNVs were generated using a two-plasmid (pWN-AB and pWN-CG) reverse genetics system of the New York 1999 strain 385-99 as described previously (7), with some modification. To produce infectious WNV, pWN-AB and pWN-CG were digested with XbaI and NgoMIV restriction enzymes, ligated at room temperature overnight, extracted with phenol-chloroform (1:1), and precipitated in 70% ethanol. For construction of recombinant WNV with single or double point mutations in NS1, the variant NS1 was subcloned from pSTBlue to pWN-AB using DraIII and XbaI restriction enzymes because the NgoMIV restriction enzyme sequence was disrupted by the introduced mutations. pWN-AB with mutant NS1 was digested with EcoRI, treated with calf intestinal phosphatase, digested with BstEII restriction enzyme, and then ligated to XbaI-BstEII-digested pWN-CG. After an overnight ligation at room temperature, pWN-AB and pWN-CG were extracted and precipitated as described above and used for DNA-dependent RNA transcription *in vitro* using an Ampliscribe T7 RNA polymerase transcription kit (Epicentre Biotechnologies) with an $m^7G(5')ppp(5')A$ RNA cap analog (New England BioLabs), followed by electroporation of BHK21 cells to generate a P-0 virus stock.

Viral growth analysis. BHK21 cells (2×10^5) were seeded into 24-well plates and infected with recombinant WNV or SINV at a multiplicity of infection (MOI) of 1 or 3, respectively, for 1 h at 37°C. Cells were washed three times with phosphate-buffered saline (PBS), and then DMEM supplemented with 2% FBS was added. Supernatants were harvested at different time points, aliquoted, and frozen at −80°C prior to titration on BHK21 cells according to published protocols (19).

Confocal microscopy. BHK21 cells grown on coverslips were infected with different SINVs, WNVs, or DENVs. For recombinant SINV, cells were infected at an MOI of 1 and stained at 14 h postinfection. For DENV and WNV, BHK21 cells were infected at an MOI of 1 and 0.1, respectively, and cells were stained at 24 h postinfection. Surface staining of NS1 was assessed with MAbs against DENV NS1 (2G6) (4) or WNV NS1 (4NS1, 9NS1, or 17NS1) (12) after incubation on ice for 30 min. Cells were washed with iced DMEM once and with iced PBS twice and then fixed with 3% paraformaldehyde in PBS for 10 min. Cov-

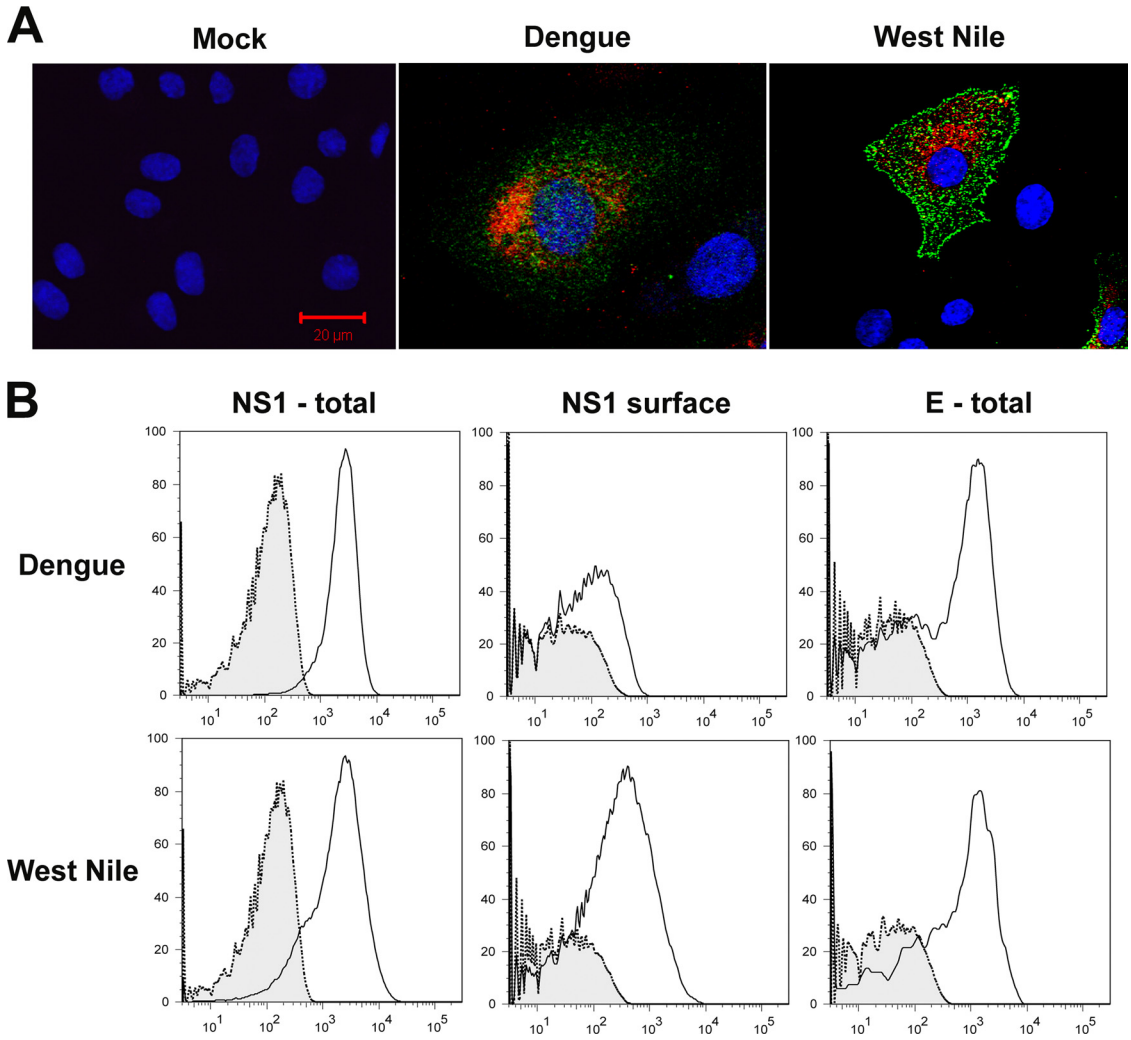

FIG. 1. Differential staining of NS1 on DENV- and WNV-infected cells. (A) Confocal microscopy. BHK21 cells were mock infected or infected with DENV (MOI of 1) or WNV (MOI of 0.1) and harvested 24 h later. A higher MOI was used for DENV to obtain the same relative level of infection as it replicates more slowly. Cells were cooled on ice and stained for NS1 on the surface using 2G6 (DENV) or 17NS1 (WNV) mouse MAbs. Subsequently, cells were fixed, permeabilized, and then stained for intracellular E protein using the cross-reactive humanized WNV E18 MAb. Nuclei were counterstained with TO-PRO-3 (blue). The images were analyzed using a LSM 510 confocal microscope. Scale bar, 20 μm. (B) Flow cytometry. BHK21 cells were infected with DENV or WNV as detailed above. Total NS1 or E was determined after cell permeabilization and indirect immunofluorescence staining with the cross-reactive MAb 9NS1 or WNV E18. Surface levels of NS1 were assessed by staining live cells at 4°C with the cross-reactive MAb 9NS1. The *y* axis indicates the number of cells, and the *x* axis shows relative NS1 or E levels. Shaded histograms are isotype controls. For microscopic and flow cytometric analyses, data are representative of at least three independent experiments.

erslips were subsequently rinsed with PBS containing 10 mM glycine, pH 7.4 (PBS/G). For staining of intracellular NS1, cells were permeabilized with PBS/G supplemented with 0.5% Triton X-100 for 3 min after fixation and then rinsed with PBS/G. For staining of both surface and intracellular NS1 simultaneously, chimeric human MAbs (mouse heavy and light chain variable region [V_H-V_L] and human heavy chain constant region [C_H] IgG1) recognizing WNV NS1 (ch17NS1) or E (chE18) protein or humanized anti-WNV E MAb (Hu-E16) (51) were used. Fixed cells were incubated with primary antibodies at room temperature for 20 min, followed by extensive washing with PBS/G. Alexa Fluor-488 goat anti-mouse IgG (Molecular Probes) or Alexa Fluor-555 goat anti-human IgG (Molecular Probes) was used as secondary antibody to detect surface and internal NS1 or E. Nuclei were counter-stained with TO-PRO-3 (Molecular Probes). Images were acquired with a laser scanning confocal microscope (Zeiss LSM 510 META; Zeiss Thornwood, NY) and analyzed with LSM image browser software (Zeiss).

Flow cytometry. To quantify surface and intracellular NS1 expression levels, flow cytometry was utilized. BHK21 cell monolayers were infected with SINV-NS1 (MOI of 1), WNV (MOI of 0.1), and DENV (MOI of 1). At 14 h (SINV) or 30 h (WNV or DENV) postinfection, infected cells were detached with Hank's balanced salt solution (HBSS) containing 5 mM EDTA. Cells were washed twice with iced PBS and incubated for 1 h on ice with the primary MAbs described above. For surface staining, after extensive washing with iced PBS, cells were fixed with 4% paraformaldehyde in PBS for 7 min and then washed with HBSS. For intracellular staining, cells were permeabilized with 0.1% (wt/vol) saponin and 0.5% bovine serum albumin (BSA) in HBSS and then incubated with the primary MAbs described above for 1 h. To detect SINV envelope proteins, we used anti-SINV mouse ascites fluid (V-560-701-562; ATCC). Cells were incubated with Alexa Fluor-647-conjugated goat anti-mouse IgG (Molecular Probe) for 30 min and then washed three times. Expression levels of NS1 and E were determined by flow cytometry on a BD FACSArray (Becton Dickinson), and data were processed with FlowJo software (Tree Star, Inc.).

Phagocytosis assay. BHK21 cells were infected with WNV at an MOI of 0.1 to 0.5 and harvested at 30 h postinfection with HBSS supplemented with EDTA. Cells were washed twice with PBS and divided into two aliquots. One set was fixed and stained for flow cytometry analysis to confirm infection and expression of NS1; the other was labeled with 5 nM carboxyfluorescein succinimidyl ester

(CFSE) (Molecular Probes) in PBS for 5 min on ice. FBS (10% final concentration) was added to quench staining, and free CFSE was removed by washing with PBS. Cells were fixed with 1% paraformaldehyde in PBS for 5 min to prevent subsequent adherence to culture dishes. After fixation, cells were opsonized with either 20 μg/ml of anti-WNV MAb 10NS1 or an isotype control antibody on ice for 1 h. Free MAb was removed after three washes with PBS. Activated macrophages were elicited by peritoneal lavage of mice that were primed with 2 ml of 4% (wt/vol) thioglycolate medium 3 days prior. Macrophages were washed with lavage medium (50 mM HEPES, 0.3% BSA, heparin [1 unit/ml], penicillin, streptomycin in PBS) and then seeded (6×10^5 cells) with DMEM containing 10% FBS overnight in individual wells of a six-well tissue culture plate. Virus-infected, carboxyfluorescein succinimidyl ester (CFSE)-labeled, fixed, and opsonized BHK21 cells were coincubated with macrophages for 2 h at 37°C. Cells were washed twice with PBS to remove unattached BHK21 cells, fixed with 2% paraformaldehyde in PBS for 10 min, and washed three additional times with PBS, and then macrophages were stained with allophycocyanin (APC)-conjugated rat anti-mouse CD11b MAb (BD Pharmingen) for 1 h on ice. After three washes with PBS, the number of macrophages with internalized BHK21 cells was evaluated by confocal microscopy.

NS1 purification and N-terminal amino acid sequencing. Recombinant wild-type or mutant NS1 was expressed in BHK21 cells using recombinant SINV. Within 24 h of infection, the supernatant was harvested, clarified by centrifugation (3,000 rpm for 10 min), filtered through a 0.2-μm-pore-size filter, and passed over a 9NS1-Sepharose immunoaffinity column. After extensive washing with 150 mM NaCl and 25 mM Tris, pH 7.4, NS1 was eluted with 10 mM diethanolamine (pH 11). The eluate was concentrated, and buffer was exchanged into 150 mM NaCl–25 mM Tris (pH 7.4) using an Amicon ultracentrifugal filter unit (Millipore). Purified NS1 was separated on 12% NuPAGE (Invitrogen) and transferred to polyvinylidene difluoride (PVDF) membrane. After band excision, N-terminal amino acid sequencing of NS1 was performed commercially (Midwest Analytical).

Sodium chlorate treatment of BHK21 cells. Sulfation and cell surface display of glycosaminoglycans were inhibited by sodium chlorate treatment (6). BHK21 cells were cultured in sulfate-free Joklik Modification Minimum Essential Medium Eagle (Sigma) supplemented with 10% dialyzed FBS (Sigma) and 10 mM sodium chlorate. After an overnight culture, cells were processed for WNV NS1 binding as described previously (5) or infected with WNV and cultured in sulfate-free medium supplemented with 10 mM sodium chlorate. Infected cells were analyzed for surface or intracellular expression of NS1 as described above.

Statistical analysis. Data sets were compared using a two-tailed, unpaired *t* test or a one-way analysis of variance (ANOVA). Data analysis was performed using Prism software (GraphPad Software).

RESULTS

WNV and DENV NS1 proteins differ in surface expression patterns. Flavivirus NS1 contains a signal sequence comprised of ~25 amino acids of the C terminus of the E gene (23), is synthesized at the ER, transported through the *trans*-Golgi network, and is displayed on the cell surface or secreted as a soluble oligomer into the extracellular milieu. Although studies have reported that the NS1 of different flaviviruses accumulate in the extracellular space at various levels (2, 10, 37, 43), the relationship and functional consequences of cell surface and secreted NS1 remain unclear, and whether targeting signals exist that facilitate preferential expression in different compartments is unknown. To begin to understand how NS1 is targeted to the cell surface, we compared plasma membrane expression patterns of NS1 from two different flaviviruses. BHK21 cells were infected with DENV serotype 2 (DENV-2) and WNV; of note, a higher multiplicity of infection (MOI of 1 compared to 0.1) for DENV was required to achieve equivalent infection due to its lower rate of replication. At ~30 h postinfection, infected cells were incubated with WNV- and DENV-specific NS1 mouse MAbs (4NS1 and 2G6, respectively) on ice, and after washing and fixation, cells were permeabilized and stained additionally with an anti-E protein cross-reactive MAb (humanized WNV E18) to allow comparison of rates of infection of the two viruses. Interestingly, the surface expression patterns varied when analyzed by confocal microscopy. DENV-infected cells showed a distinct NS1 stain-

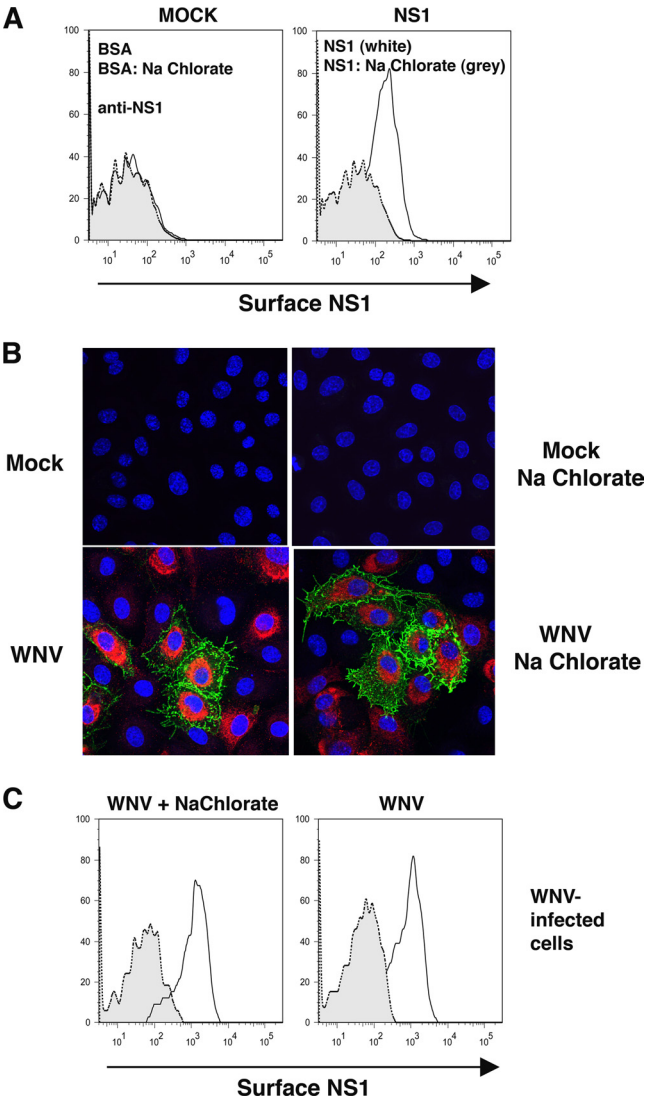

FIG. 2. NS1 on the surface of flavivirus-infected cells is targeted directly to the plasma membrane. (A) Sodium chlorate inhibits binding of soluble NS1 to uninfected cells. Uninfected BHK21 cells were pretreated with medium or medium supplemented with 10 mM sodium chlorate, which inhibits the surface expression of glycosaminoglycans (5), and then incubated with soluble WNV NS1 for 2 h at 4°C. Cells were washed extensively and stained for NS1 on the surface using the 9NS1 MAb. (B and C) Sodium chlorate does not inhibit surface expression of NS1 on WNV-infected cells. BHK21 cells were infected with WNV (MOI of 0.1) or treated with medium or medium supplemented with 10 mM sodium chlorate, and 1 day later live cells were immunostained on ice with 9NS1 (B) or 4NS1 (C) MAb to determine the levels of surface NS1 by confocal microscopy (B) or flow cytometry (C). Subsequently, for panel B the same cells were fixed, permeabilized, and stained with chimeric human 17NS1 MAb to confirm the total levels of NS1. For the flow cytometry data, the *y* axis indicates the number of cells, and the *x* axis shows relative NS1 levels. Shaded histograms are isotype controls. The data are representative of two independent experiments.

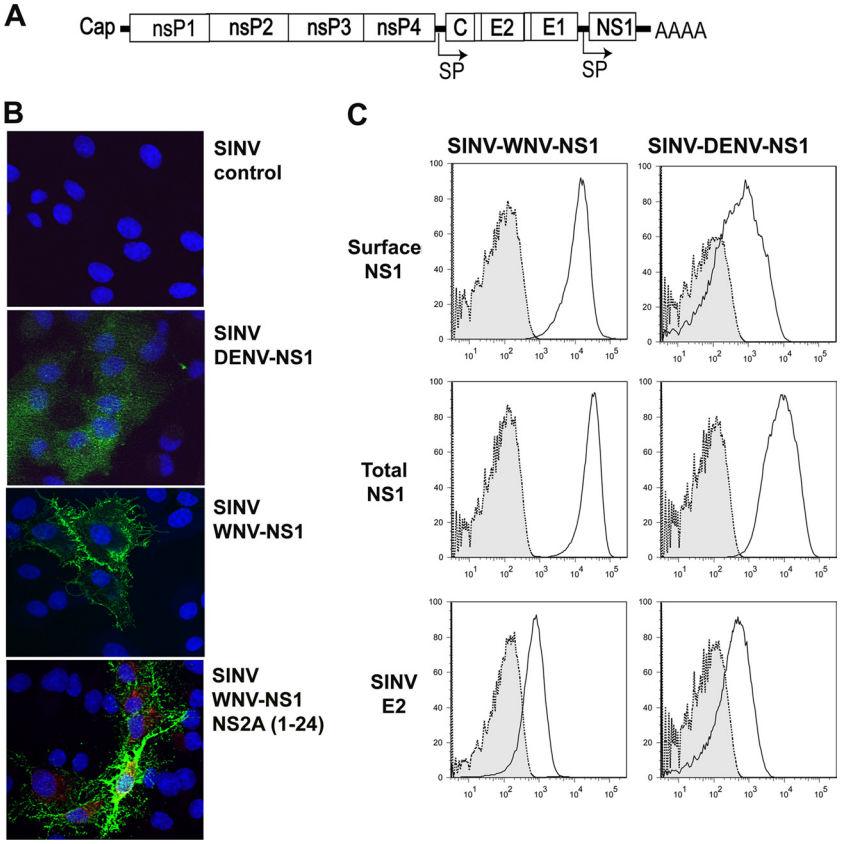

FIG. 3. Expression of DENV and WNV NS1 in BHK21 cells using a recombinant infectious SINV. (A) Scheme of transgenic expression of NS1. Full-length DENV or WNV NS1 was cloned downstream of a second subgenomic 26S promoter as indicated in the cartoon. Transfection of *in vitro* derived RNA produces infectious SINV that encodes a flavivirus NS1 transgene. (B) Confocal microscopy. BHK21 cells were mock infected or infected with SINV-DENV-NS1, SINV-WNV-NS1, or SINV-WNV-NS1-NS2A$_{1\text{-}24}$ (MOI of 0.1) and harvested at 14 h after infection. Live cells were cooled to 4°C and stained for NS1 on the surface using the cross-reactive 9NS1 MAb. Nuclei were counterstained with TO-PRO-3. A lower MOI was used in the microscopic experiments to facilitate visualization of individual infected cells. (C) Flow cytometry. BHK21 cells were infected with SINV-DENV-NS1 or SINV-WNV-NS1 at an MOI of 1 as detailed above. Total DENV NS1, WNV NS1, and SINV envelope proteins were determined after cell permeabilization and indirect immunofluorescence staining with the cross-reactive MAb 9NS1 or anti-SINV mouse ascites fluid. Surface NS1 levels were assessed by staining live intact cells at 4°C. The *y* axis indicates the number of cells, and the *x* axis shows relative NS1 and E2 levels. Shaded histograms are isotype controls. The data are representative of at least three independent experiments.

ing pattern on the plasma membrane surface compared to that observed in WNV-infected cells (Fig. 1A). This difference was not an artifact of the specific MAbs used as it was reproduced with several anti-DENV (1F11 and 1B10) or anti-WNV (17NS1 and 10NS1) NS1 antibodies and with a cross-reactive anti-NS1 MAb (9NS1) that recognizes both WNV and DENV NS1 equivalently (data not shown).

To determine if the confocal microscopy expression patterns were related to the levels of surface NS1 on WNV- and DENV-infected cells, we analyzed cells more quantitatively by flow cytometry (Fig. 1B). Although the extents of WNV and DENV infections were similar, as judged by staining of total E and NS1 proteins in permeabilized cells with the cross-reactive MAbs WNV E18 and 9NS1, respectively, the surface expression of NS1 on infected BHK cells varied. WNV infection resulted in greater surface expression of NS1 (increased percentage of positive cells and higher mean fluorescence intensity) than in cells infected with DENV, even when the same MAb (9NS1) was used for direct comparison (Fig. 1B, middle panels). Thus, WNV infection results in the accumulation of more NS1 on the cell surface in a distinct morphological pattern.

Cell surface NS1 on infected cells is targeted directly to the plasma membrane. A previous study showed that soluble DENV can bind back to the cell surface of uninfected cells through interactions with glycosaminoglycans displaying heparan and chondroitin sulfate E moieties (5). To assess whether NS1 on the plasma membrane surface of infected cells reflected the binding back of soluble NS1, BHK21 cells were infected with WNV and treated with 10 mM sodium chlorate, which inhibits the surface expression of glycosaminoglycans (6), and then analyzed by flow cytometry for surface NS1. Importantly, treatment of uninfected cells with sodium chlorate abolished binding of soluble WNV NS1 to the cell surface (Fig. 2A, right panel), as seen previously with DENV (5). However, sodium chlorate treatment did not appreciably alter the expression pattern or level of NS1 on WNV-infected (Fig. 2B and C) or DENV-infected cells (5; also data not shown). Thus, NS1 on the plasma membrane of infected BHK21 cells largely reflects a pool transported from within cells and not

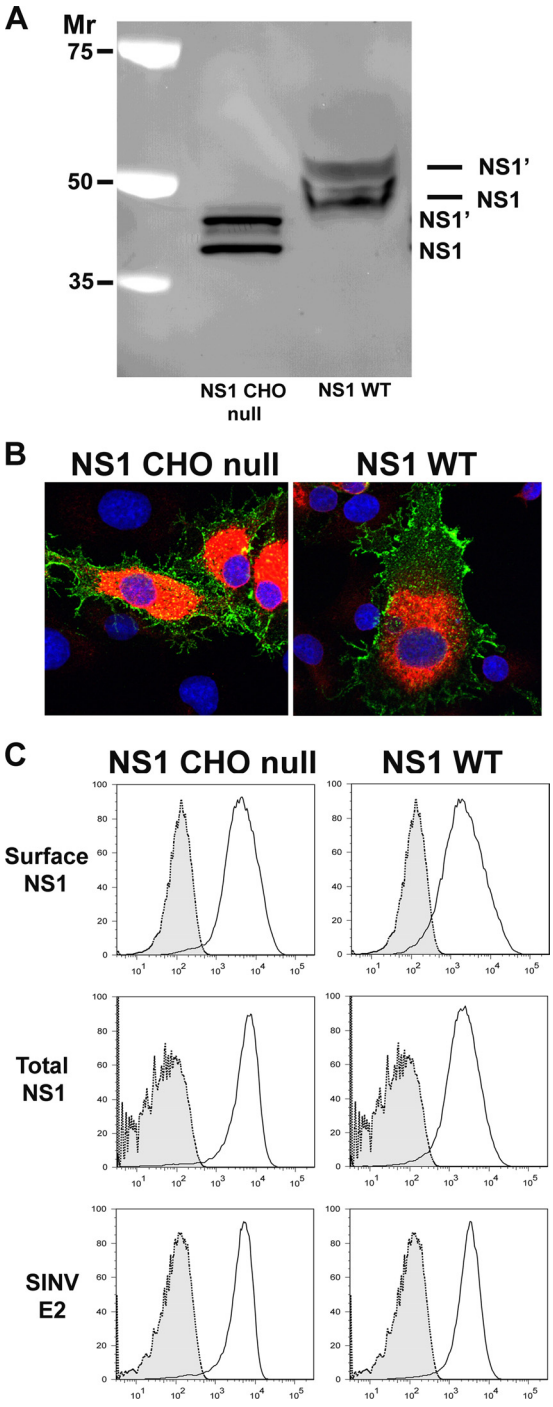

FIG. 4. The effect of N-linked glycosylation on cell surface expression of NS1 using a recombinant infectious WNV or transgenic SINV. A glycosylation null mutant of WNV NS1 (CHO null) was generated by iterative site-directed mutagenesis in a shuttle vector and then cloned into the infectious cDNA of a New York 1999 strain (385-99) of WNV. (A) BHK21 cells were infected with WNV expressing wild-type NS1 (MOI of 0.1) or NS1 CHO null (MOI of 3) and subjected to Western blotting with 8NS1 MAb under reducing conditions. A higher MOI was required for the CHO null WNV because of a growth defect of this virus, as reported previously (62). The difference in NS1 size of the CHO null mutant is due to the absence of N-linked glycans. Both wild-type and mutant NS1s have additional higher-molecular-weight NS1′ forms, which are indicated and are due to ribosomal frameshifting (25, 47). (B) Confocal microscopy. BHK21 cells were infected with wild-type or NS1 CHO null WNV and harvested at 24 h after infection. Live cells were cooled to 4°C and stained for NS1 on the surface using the cross-reactive 9NS1 MAb (green). Subsequently, cells were fixed and permeabilized and stained with chimeric human 17NS1 MAb to confirm expression of NS1 (red). Nuclei were counterstained with TO-PRO-3. (C) Flow cytometry. BHK21 cells were infected with SINV-WNV-NS1 CHO null or SINV-WNV-NS1 as detailed in the legend of Fig. 2 and harvested at 14 h after infection. Total WNV NS1 or SINV E2 was determined after cell fixation, permeabilization, and indirect immunofluorescence staining. Surface NS1 levels were assessed by staining live intact cells at 4°C. The *y* axis indicates the number of cells, and the *x* axis shows relative NS1 levels. Shaded histograms are isotype controls. The data are representative of at least three independent experiments.

one that was secreted and bound back to surface glycosaminoglycans.

Ectopic expression of DENV and WNV NS1 in Sindbis viruses recapitulates phenotypic differences. To eliminate the possibility that the expression pattern variation was related to the differences in infectivity, we expressed DENV and WNV NS1 ectopically using a double subgenomic Sindbis virus (SINV) (53, 55). The complete DENV (amino acids 1 to 352) and WNV (amino acids 1 to 352) NS1 genes were cloned downstream of their respective 24- or 25-amino-acid leader sequences (C terminus of the E gene) and a second 26S subgenomic promoter of SINV (Fig. 3A). Infectious RNA was transcribed from cDNA *in vitro* and electroporated into BHK21 cells, and recombinant SINV expressing WNV NS1 (SINV-WNV-NS1) or DENV NS1 (SINV-DENV-NS1) was harvested. Single-step growth analysis of recombinant SINV expressing WNV or DENV NS1 showed growth kinetics similar to the kinetics of recombinant SINV with NS1 cloned in the opposite orientation, confirming that expression of flavivirus NS1 did not affect SINV replication (data not shown).

To compare the surface expression pattern of ectopically expressed NS1, BHK21 cells were infected with SINV-WNV-NS1 and SINV-DENV-NS1 at equivalent MOIs and analyzed. By confocal microscopy, the expression pattern on the plasma membrane of SINV-WNV-NS1- or SINV-DENV-NS1-infected cells largely recapitulated that observed with the parent flaviviruses (Fig. 3B). The amount of NS1 on the surface of SINV-WNV-NS1-infected cells was substantially (~20-fold) greater than that of SINV-DENV-NS1 as judged by flow cytometry (Fig. 3C), even though total levels of WNV and DENV NS1 or SINV E2 protein in permeabilized cells were only slightly (<3-fold) different. Similar phenotypic expression patterns were observed with BHK21 cells that propagated the DENV or WNV subgenomic replicon or that were transfected with plasmid DNA encoding NS1 (data not shown). These results suggest that the surface expression pattern was an inherent characteristic of WNV or DENV NS1 and not biased by the differential replication rates of the viruses. Moreover, the surface expression pattern of WNV NS1 did not differ after inclusion of the N-terminal 24 amino acids of NS2A (Fig. 3B), which has been suggested with respect to DENV to encode a noncanonical glycosyl-phosphatidylinositol (GPI) anchor (30).

Targeting of WNV NS1 to the plasma membrane is not affected by N-linked glycosylation. To begin to dissect the requirements for targeting of flavivirus NS1 to the plasma

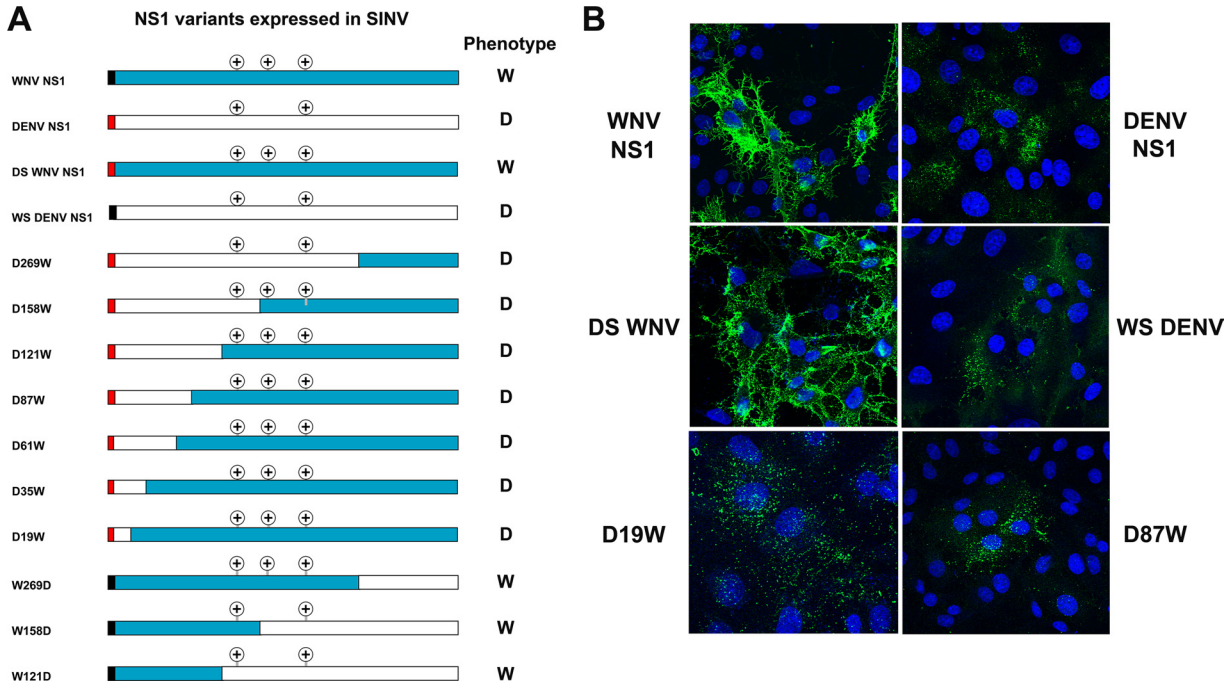

FIG. 5. Scheme and phenotypes of the WNV-DENV NS1 chimeras. (A) The construction and expression of NS1 chimeras are detailed in Materials and Methods. The most N-terminal box indicates the origin of the signal peptide (black, WNV NS1; red, DENV NS1). The remaining boxes denote the regions that are comprised of WNV NS1 (blue) or DENV NS1 (white). The numbers correspond to the amino acid position of NS1 at the breakpoint of the chimera. Encircled plus signs denote encoded N-linked glycosylation sites; wild-type DENV and WNV NS1s have two and three N-linked glycans, respectively. The surface expression phenotype for each NS1 variant, when expressed in a recombinant SINV, is listed immediately to the right of the chimera: W and D indicate a WNV-like or DENV-like surface pattern, respectively. The analysis is based on at least three independent experiments with each chimera. (B) Confocal microscopy. BHK21 cells were infected with SINV-WNV-NS1 (WNV NS1), SINV-DENV NS1 (DENV NS1), or the indicated chimera (MOI of 0.1) and harvested at 14 h after infection. Live cells were cooled to 4°C and stained for NS1 on the surface using the cross-reactive 9NS1 MAb. Nuclei were counterstained with TO-PRO-3. The data are representative of two or three independent experiments.

membrane, we assessed the effect of N-linked glycosylation on surface expression. We evaluated this phenotype as previous studies suggested that loss of N-linked glycans on NS1 affects infectivity of different flaviviruses (15, 48, 62). WNV NS1 has three N-linked glycans (amino acids 130, 175, and 207), whereas DENV NS1 has two (amino acids 130 and 207). To examine whether N-linked glycosylation affects the surface expression pattern of WNV NS1, we generated asparagine-to-alanine mutations within the three consensus N-linked glycan sites (Fig. 4A). This glycosylation-null triple mutant WNV NS1 was introduced into both the SINV expression system and an infectious cDNA clone of WNV New York 1999 (7). In either system, NS1 lacking N-linked glycans showed a surface pattern and level that were similar to those of the wild-type NS1, as determined by confocal microscopy and flow cytometry (Fig. 4B and C; also data not shown). Thus, it appears unlikely that the additional N-linked glycan at amino acid 175 of WNV explains the differential surface expression patterns of WNV and DENV NS1s.

The N-terminal region of NS1 regulates the surface expression phenotype. To define the basis for the differential surface expression patterns of WNV and DENV NS1, we generated a series of NS1 chimeras (Fig. 5A). We initially examined whether the respective signal peptides of DENV and WNV NS1s modulated surface expression patterns using several MAbs (e.g., 2G6, 4NS1, 17NS1, and 9NS1) that recognize different regions of DENV or WNV NS1. Notably, swapping the signal peptides (DS WNV and WS DENV) did not appreciably alter surface expression, establishing that this motif does not determine differential surface targeting of NS1 (Fig. 5B, middle panels). Chimeras containing the 19 amino acids of DENV NS1 C-terminal to the signal sequence cleavage position, however, conferred a DENV NS1-like surface expression pattern on WNV NS1, as judged by confocal microscopy (Fig. 5B, bottom panels). Alignment of the amino acid sequences of WNV and DENV NS1s downstream of the signal peptide revealed a region with significant diversity (Fig. 6A). To test whether any of these residues was responsible for the phenotype, four sets of 2-amino-acid changes corresponding to the DENV sequences were introduced into WNV NS1 and expressed in recombinant SINV. Changes at amino acid positions 5 and 6 (AI5VV), 6 and 7 (ID6VS), and 8 and 9 (IS8WK) had subtle effects on decreasing or increasing WNV NS1 surface expression and distribution (Fig. 6B and C). However, a change of WNV RQ to DENV NK at amino acid positions 10 and 11 (RQ10NK) switched the WNV NS1 expression pattern to one that resembled DENV NS1 with markedly reduced surface expression. Further mutational analysis revealed that a single amino acid substitution (R → N) at position 10 was sufficient to modulate the targeting pattern of WNV NS1 (Fig. 6B). This amino acid is noteworthy as all four serotypes of DENV differ from the remainder of viruses within the genus at this site (Fig.

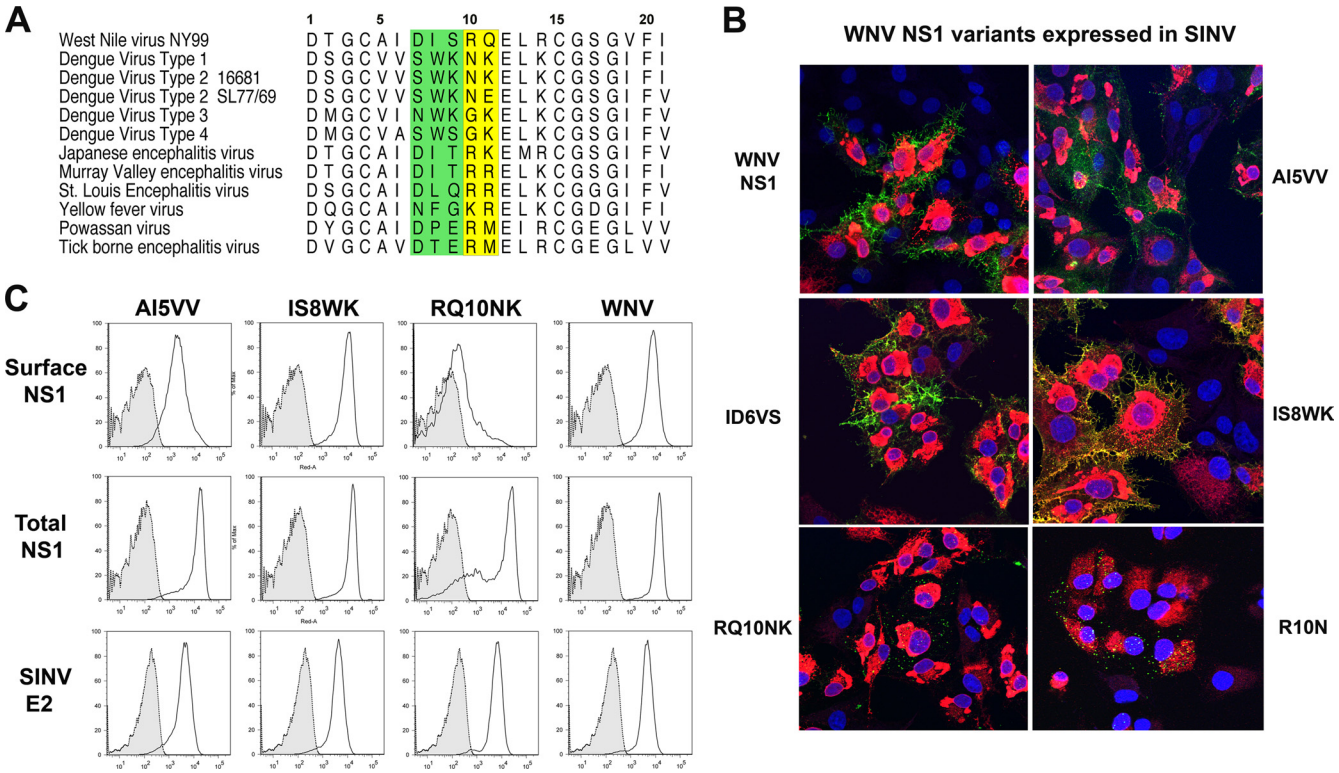

FIG. 6. Phenotype of site-specific variants in the N-terminal region of NS1. (A) Sequence alignment of flavivirus NS1 immediately C-terminal to the signal peptide cleavage site. The numbers above correspond to the amino acid sequence of NS1. The sequences highlighted in green and yellow comprise a region of dissimilarity between the two viruses. Residue 10 shows significant variation between all serotypes of DENV and other flaviviruses. (B) Confocal microscopy. BHK21 cells were infected with SINV-WNV-NS1 (WT) or a series of mutants (AI5VV, ID6VS, IS8WK, RQ10NK, and R10N) that incorporated the corresponding residues of DENV NS1 and harvested at 14 h after infection. Cells were cooled to 4°C and stained for NS1 on the surface using the 4NS1 MAb (green). Subsequently, cells were fixed and permeabilized and stained with chimeric human 17NS1 MAb to confirm expression of NS1 (red). Nuclei were counterstained with TO-PRO-3. The data are representative of two to three independent experiments. (C) Flow cytometric analysis. BHK21 cells were infected with SINV-WNV-NS1 or the indicated mutants as detailed above. Staining of live intact cells at 4°C assessed the surface levels of wild-type and variant NS1 using the 4NS1 MAb. Total NS1 and SINV E2 were determined after fixation, cell permeabilization, and immunofluorescence staining with anti-NS1 or anti-SINV E2 antibodies. The *y* axis indicates the number of cells, and the *x* axis shows the relative NS1 or E2 level. Shaded histograms are isotype controls. Data are representative of at least three independent experiments.

6A), with none of the DENV strains containing basic charged (R or K) residues. Consistent with this region being important for targeting of NS1, a reciprocal change of DENV NK to WNV RQ at amino acid positions 10 and 11 (NK10RQ) switched the NS1 expression pattern of DENV-2 to one that resembled that of WNV NS1 with increased surface expression (Fig. 7A and B).

Surface expression and secretion of NS1 are inversely correlated. To assess whether the different surface expression patterns of wild-type and variant NS1 were associated with alterations in intracellular trafficking or posttranslational modification, pulse-chase studies were undertaken. BHK21 cells were infected with different SINV NS1 for 12 h, pulsed with [^{35}S]cysteine-methionine for 20 min, and chased for various times. Cell lysates and supernatants were immunoprecipitated and digested with endoglycosidase H (endo H), which removes high-mannose-content sugars, or peptide N-glycosidase F (PNGase F), which cleaves all sugar moieties from high mannose, hybrid, and complex oligosaccharides from N-linked glycoproteins. Notably, wild-type, IS8WK, and RQ10NK NS1, which had distinct surface patterns of expression, exhibited relatively similar intracellular levels at early (e.g., 1 h) chase times (Fig. 8A and B). However, at later chase times (e.g., 6 h), the level of intracellular RQ10NK NS1 was reduced in cell lysates and retained sensitivity to endo H treatment, whereas wild-type and IS8WK NS1 acquired complex/hybrid sugars during Golgi compartment transit and became partially resistant to endo H digestion (Fig. 8B, left panel). Two independent experiments established that acquisition of complex/hybrid sugars in the Golgi compartment was not necessary for cell surface expression of NS1 and, thus, did not explain the phenotype observed with the RQ10NK variant: (i) the NS1 glycosylation null mutant had normal surface expression both by flow cytometry and confocal microscopy (Fig. 4), and (ii) treatment of cells propagating a Venezuelan equine encephalitis replicon that transgenically expressed wild-type WNV NS1 (VEE-NS1) with deoxymannojirimycin, which inhibits processing of high-mannose sugars, also did not affect surface expression levels (Fig. 8C and D).

The pulse-chase analysis of the SINV-NS1-infected cell supernatants suggested a reciprocal relationship between the level of surface expression and secretion of NS1. Chimeras

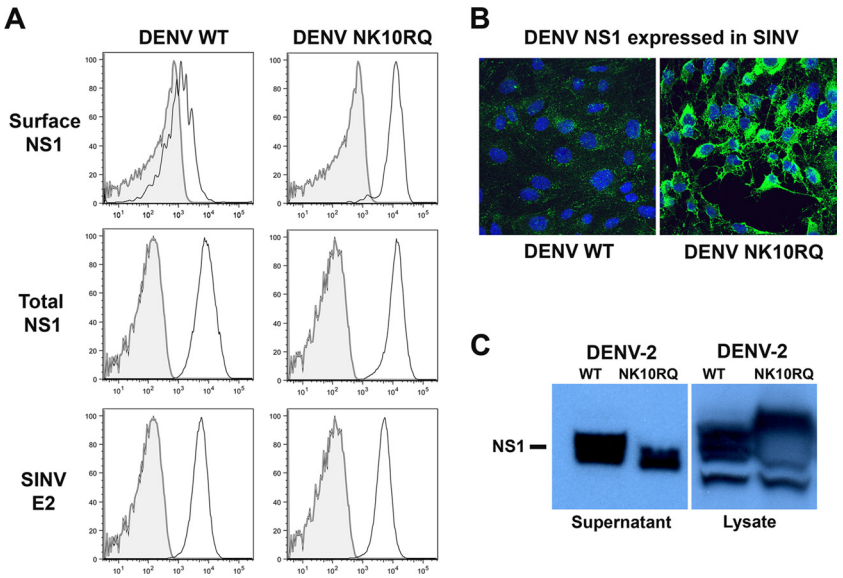

FIG. 7. Phenotype of site-specific variants in the N-terminal region of DENV-2 NS1. (A) Flow cytometric analysis. BHK21 cells were infected with SINV-DENV-2 wild-type (WT) NS1 or the mutant SINV-DENV-2 NK10RQ that incorporated the corresponding residues of WNV NS1. Staining of live intact cells at 4°C assessed the surface levels of wild-type and variant NS1 using the cross-reactive 9NS1 MAb. Total DENV NS1 and SINV E2 were determined after fixation, cell permeabilization, and immunofluorescence staining with anti-NS1 or anti-SINV E2 antibodies. The *y* axis indicates the number of cells, and the *x* axis shows relative DENV NS1 or SINV E2 level. Shaded histograms are isotype controls. Data are representative of at least two independent experiments. (B) Confocal microscopy. BHK21 cells were infected with SINV-DENV-2 WT NS1 or the mutant SINV-DENV-2 NK10RQ and harvested at 14 h after infection. Cells were cooled to 4°C and stained for NS1 on the surface using the 9NS1 MAb (green). Nuclei were counterstained with TO-PRO-3. The data are representative of two independent experiments. (C) Western blotting with the 1F11 anti-DENV-2 NS1 MAb of supernatants and cell lysates from BHK21 cells infected with SINV-DENV-2 WT NS1 or SINV-DENV-2 NK10RQ. Note that the levels of NS1 in the supernatant of the SINV-DENV-2-NK10RQ samples are lower and that those in the cell lysate are slightly higher.

with N-terminal 19 amino acids of DENV NS1 or the site-specific RQ10NK variant showed enhanced accumulation in the supernatants (Fig. 8B right panel, and 9B; also data not shown). Analogously, the DENV-2 NK10RQ variants showed diminished levels in the supernatant despite the increased surface expression (Fig. 7C). Consistent with this, wild-type DENV NS1 appeared in the supernatant at earlier chase times than WNV NS1 (Fig. 9A, bottom panel), and similar to the RQ10NK WNV mutant, at later chase times (e.g., 6 h) the levels of intracellular DENV NS1 were reduced in cell lysates (Fig. 9A, top panel). All wild-type and variant NS1 in cell supernatants, including the RQ10NK mutant, were present in a partially endo H-resistant form (Fig. 8A and D). In contrast, the glycosylation null mutant of WNV NS1 was secreted at very low levels (data not shown). Because treatment of cells propagating the VEE-NS1 replicon with deoxymannojirimycin did not markedly affect levels of NS1 in the supernatant, the presence rather than modification of the N-linked glycans appears required for efficient secretion (Fig. 8D, left panel). Overall, these experiments demonstrate that variants of WNV NS1 (e.g., RQ10NK) that exhibited a DENV-like cell surface pattern were secreted at higher levels, establishing an inverse correlation between surface expression and secretion of NS1. Moreover, surface expression of NS1 did not require N-linked glycans whereas secretion did, but for the latter, the conversion to hybrid/complex sugars was not essential. Consistent with this, introduction of the RQ10NK mutation into the glycosylation null WNV NS1 variant failed to substantially increase secretion (data not shown).

N-terminal amino acid sequencing of secreted NS1. Our experiments demonstrated that site-specific amino acid changes in the N-terminal region of WNV NS1 protein decreased surface expression yet increased secretion. We hypothesized that this could be due to an altered interaction with an unknown moiety on the plasma membrane, or, because the mutations were so close to the N terminus, preferential use of a downstream signal peptide sequence might favor secretion. Computational prediction algorithms suggested that the introduction of DENV NS1 sequences at amino acid 8 to 10 of WNV NS1 might alter the hydrophobicity of the region, rendering the variant proteins susceptible to a downstream signal cleavage event (data not shown). To evaluate whether the introduction of DENV NS1 amino acid sequences affected the N terminus of the protein, variant NS1 (AI5VV and RQ10NK) were harvested from supernatants of SINV-NS1-infected cells, purified, and evaluated by direct N-terminal amino acid sequencing. As the two variant NS1 contained the predicted N-terminal 4 amino acids corresponding to the wild-type protein (D-T-G-C), altered surface expression and secretion were not explained by a change in the location of signal peptide cleavage site.

NS1 secretion inversely correlates with viral replication. To address whether the N-terminal amino acids that regulated NS1 surface expression and secretion in the SINV expression system similarly controlled its cellular distribution in the context of infectious WNV, the AI5VV, ID6VS, IS8WK, and RQ10NK mutations were introduced into the infectious WNV New York 1999 cDNA clone (7), and recombinant viruses were recovered. Most mutants showed similar plaque sizes and

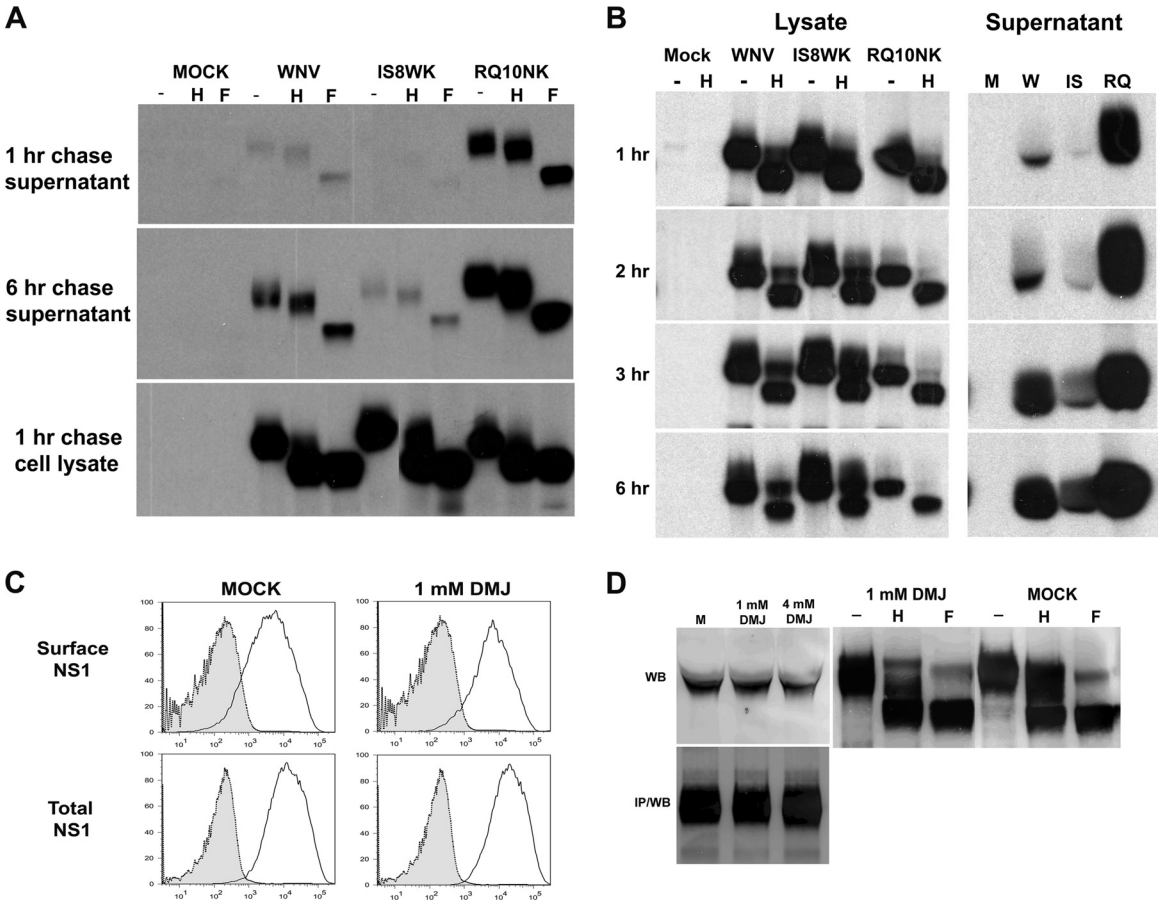

FIG. 8. Biosynthesis of wild-type and nutant WNV NS1. (A) BHK21 cells were infected with different SINV-NS1 for 12 h, placed in cysteine-methionine-free medium for 20 min, pulsed with [^{35}S]cysteine-methionine for 20 min, and then chased for 1 or 6 h. Cell supernatants or lysates were harvested, immunoprecipitated with 9NS1 MAb-Sepharose, and digested with endo H (H) or PNGase F (F). (B) A more detailed early ^{35}S pulse-chase time course was performed with wild-type NS1, IS8WK, and RQ10NK with recombinant SINV. Cell supernatants or lysates were harvested, immunoprecipitated with 9NS1 MAb-Sepharose, and digested with endo H (H). (C and D) The effect of processing high-mannose (Man9GlcNAc2) N-linked glycans on intracellular levels, surface expression, and secretion of NS1. BHK21 cells propagating a VEE replicon that expresses a WNV NS1 transgene were mock treated (M) or incubated with 1 or 4 mM deoxymannojirimycin (DMJ) overnight, which inhibits processing of high-mannose sugars. The VEE-NS1 replicon was used as a transgenic expression system because (i) it expresses NS1 at high levels in a stable fashion, and (ii) its replication is not altered by inhibitors of N-linked glycan processing. Cells were subjected to surface and intracellular staining of NS1 by flow cytometry (C) and Western blotting (D, top left [WB]) or immunoprecipitation (IP) of cell supernatants (bottom left panel) and endo H (H) or PNGase F (F) treatment of cell supernatants after immunoprecipitation (middle and right panels).

single-step growth kinetics compared to the parent strain (Fig. 10A and B). However, the RQ10NK mutant, which showed decreased surface expression and increased secretion of NS1 (Fig. 6 and 8) in the SINV ectopic expression model, was noticeably attenuated in BHK21 cells, with smaller plaque size and impaired growth kinetics.

To address whether the RQ10NK change in WNV recapitulated the surface expression phenotype that was observed with transgenic SINV, cells were infected at a higher MOI to compensate for the growth defect so that the level of intracellular NS1 achieved was equivalent to that of the wild-type NS1. Under these conditions, the WNV RQ10NK behaved similarly to SINV RQ10NK NS1, with decreased surface expression (Fig. 10C and D). Analogously, mutations that caused more subtle phenotypes with SINV had corresponding effects in the context of infectious WNV, with decreased and increased surface expression of AI5VV and IS8WK NS1, respectively. Other mutations (e.g., Q11K) had little effect on surface distribution of levels. Overall, site-specific substitutions in the N-terminal region of WNV NS1 with the corresponding DENV NS1 amino acids altered the relative levels of surface and secreted NS1.

Independent confirmation of an effect of RQ10NK NS1 on viral growth was achieved using a *trans*-complementation assay (33) in which wild-type NS1 was expressed ectopically. We infected BHK21 cells propagating the VEE-NS1 replicon with WNV RQ10NK to determine whether exogenously expressed NS1 could rescue the attenuated growth phenotype. Notably, the small-plaque phenotype and growth defects of WNV RQ10NK were restored by transgenic expression of wild-type NS1 (Fig. 11A and B), confirming that the growth defect was due to the specific mutation in NS1. Remarkably, large-plaque revertants of WNV RQ10NK that were isolated after serial passage in culture replicated at wild-type levels, acquired N →

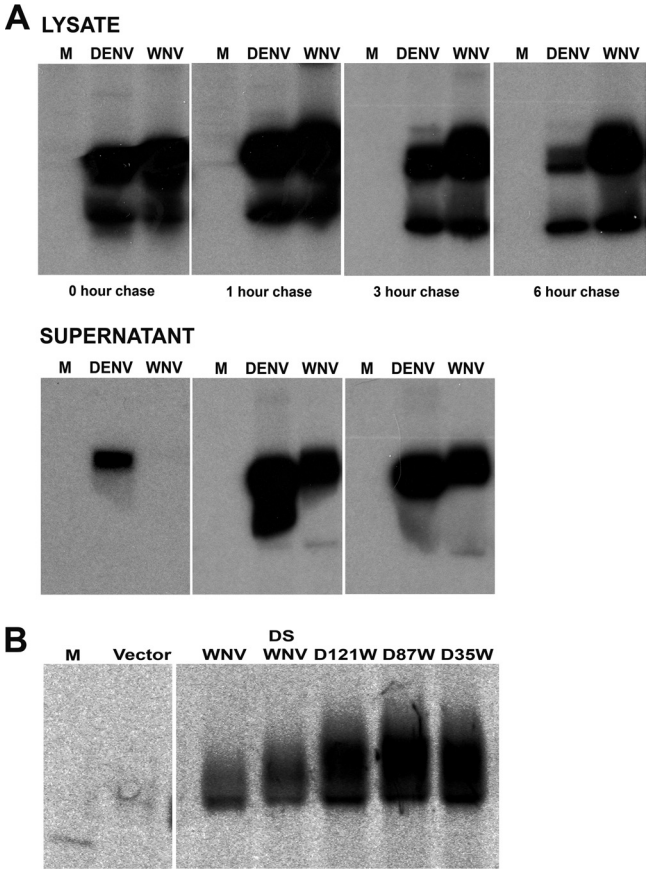

FIG. 9. Comparison of intracellular and extracellular accumulation of DENV and WNV NS1 by pulse-chase analysis. (A) BHK21 cells were infected with SINV-DENV-NS1 or SINV-WNV-NS1, labeled with [^{35}S]cysteine-methionine for 20 min, chased for the indicated times, and immunoprecipitated with cross-reactive 9NS1 MAb-Sepharose. (B) ^{35}S-labeled supernatants from mock-infected cells (M) or cells infected with SINV (Vector) or SINV expressing wild-type or chimeric (DS WNV, D121W, D87W, and D35W) NS1. Cells were infected for 12 h, pulsed with ^{35}S for 20 min, and chased for 3 h. Supernatants were harvested, immunoprecipitated with 9NS1 MAb-Sepharose, and electrophoresed. The data in this figure are representative of two to four independent experiments per panel.

R or N → K positive-charge reversions at amino acid 10 of NS1, and showed wild-type levels and patterns of expression of NS1 on the surface of infected cells (Fig. 11C, D, and E).

Targeting of NS1 alters antibody opsonization and phagocytosis. A previous study demonstrated that antibody recognition of cell surface WNV NS1 triggered Fc-γ receptor-mediated phagocytosis and viral clearance (13). To evaluate the potential impact of differential NS1 targeting, BHK21 cells were infected with wild-type and mutant WNV that induced disparate cell surface NS1 expression phenotypes. Again, because of the growth defect of the WNV RQ10NK mutant virus, a higher MOI was used for this virus to achieve equivalent infection. At 30 h, a similar level of cell infection and the distinct surface expression levels of NS1 with the different viruses were confirmed by flow cytometry (Fig. 10D). Infected BHK21 cells were labeled with carboxyfluorescein, opsonized with 10NS1 MAb, and incubated with activated peritoneal macrophages. After extensive washing and fixation, macrophages were stained with an anti-CD11b MAb and analyzed by confocal microscopy for internalization of BHK21 cells. Cells infected with the WNV RQ10NK mutant were phagocytosed by activated macrophages to a significantly lower degree (14% versus 41%' $P < 0.05$) than those infected with WNV expressing wild-type or other variant NS1 (Fig. 12).

DISCUSSION

Flavivirus NS1 is a versatile and unique nonstructural protein among RNA viruses as it is glycosylated, expressed on the cell surface, secreted into the extracellular space, and binds back to the surface of uninfected cells. Additionally, through uncertain mechanisms intracellular NS1 acts as a cofactor for viral RNA replication (33, 41) and, possibly, inhibits Toll-like receptor 3 (TLR3) signal transduction (63). Extracellular NS1 also modulates the host innate immune response by binding factor H, C1s, and C4 to promote degradation of C4 to C4b and diminish complement activation (3, 11, 36). Despite an increasing number of ascribed functions, the mechanisms that regulate NS1 distribution within, on, and outside infected cells remain unclear. Secreted NS1 can attach to the surface of uninfected cells via interactions with the glycosaminoglycans heparan sulfate and chondroitin sulfate E (5). However, this mechanism does not explain how the majority of NS1 is displayed on the surface of infected cells. Although NS1 lacks a transmembrane domain or canonical membrane-targeting signal, a subset appears to associate with the plasma membrane by glycosylphosphatidylinositol anchor and/or lipid rafts (30, 49, 50), at least for some flaviviruses. We hypothesized that a more detailed understanding of the *cis* determinants of cell surface targeting and secretion of NS1 would provide insight into its cellular distribution.

Using both flavivirus-infected BHK21 cells and an ectopic NS1 expression system, we show that DENV and WNV NS1 differentially target to the plasma membrane and extracellular space. On the plasma membrane, WNV NS1 is expressed at higher levels than DENV NS1 and in a distinct pattern, whereas DENV NS1 accumulates at lower levels than WNV NS1. Correspondingly, as judged by pulse-chase and Western blot experiments, DENV NS1 is secreted at higher levels in the cell supernatants than WNV NS1. Thus, we define a reciprocal relationship in infected mammalian cells between cell surface and secreted forms of WNV and DENV NS1. Interestingly, and in contrast to some prior studies with DENV NS1 (30, 50), our data suggest that the N-terminal 24 amino acids of NS2A ($NS2A_{1-24}$) are not required for cell surface targeting of WNV NS1: we observed the same patterns of distribution and expression of NS1 on cells infected with WNV, SINV-NS1, or SINV-NS1-$NS2A_{1-24}$. These data agree with earlier transient cDNA expression studies, which showed that JEV NS1 protein expressed in isolation was faithfully processed with respect to retention in the ER, secretion, glycosylation, membrane association, and dimerization (24). Instead, the presence of the N terminus of NS2A facilitates production of the higher-molecular-weight NS1′ species in the JEV serogroup subset of flaviviruses through a ribosomal frameshift mechanism (8, 25, 47).

Because DENV and WNV NS1 showed different cell surface patterns in the context of infection or transgenic expression, we hypothesized that they might encode distinct targeting signals.

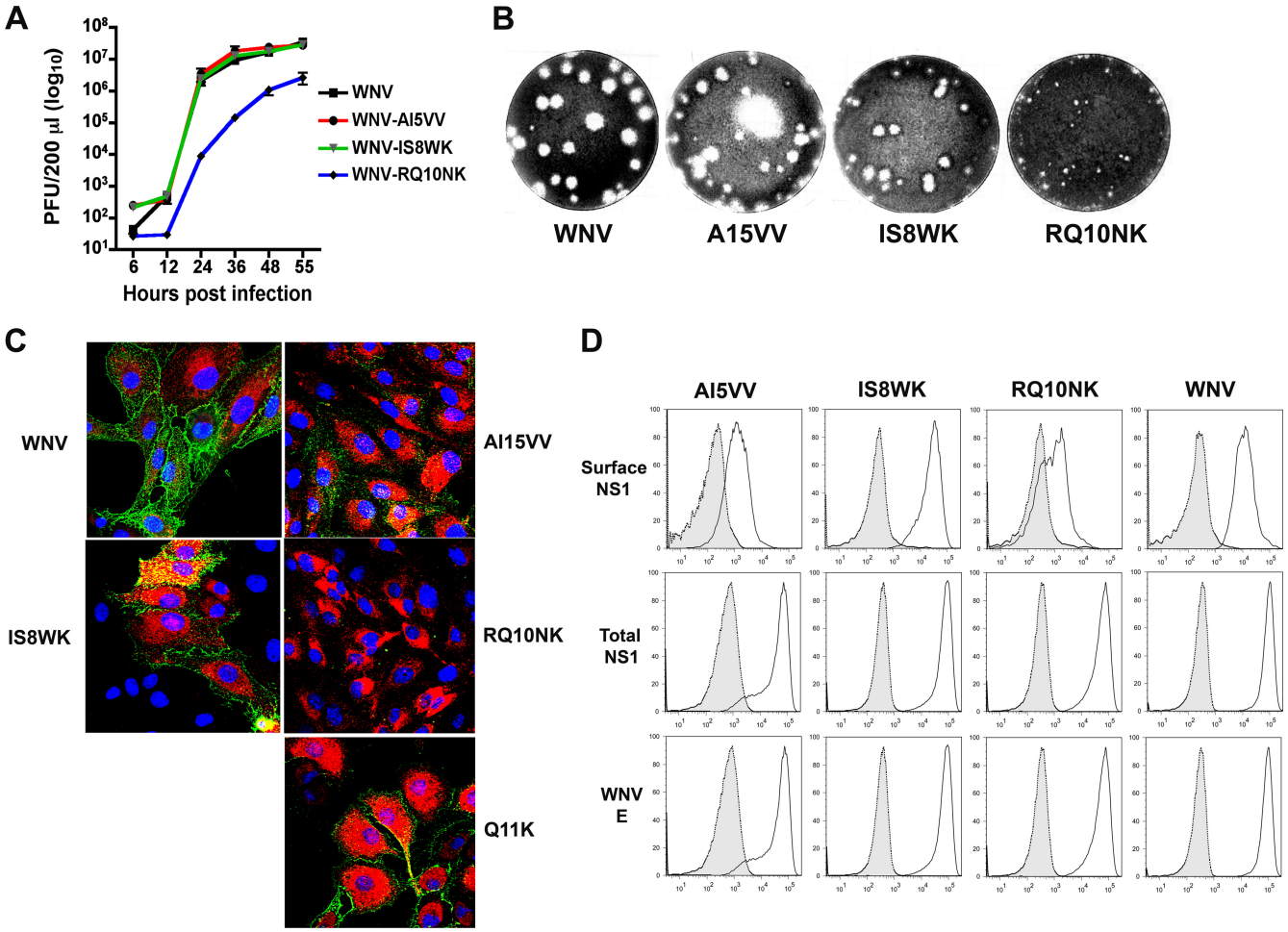

FIG. 10. Phenotype of NS1 variants after substitution into the infectious clone of WNV. (A) Growth curve kinetics of recombinant WNV (wild type, AI5VV, IS8WK, and RQ10NK) in BHK21 cells. Cells were infected and harvested at the indicated times, and virus was titrated by plaque assay. Data are representative of three independent experiments. (B) Plaque size phenotype of different NS1 variants in the context of the infectious WNV clone. Note the small-plaque phenotype of the RQ10NK NS1 variant. (C) Confocal microscopy. BHK21 cells were infected with recombinant wild-type WNV or a series of mutants (AI5VV, IS8WK, RQ10NK, and Q11K) that incorporated the corresponding residues of DENV NS1 and were harvested at 30 h after infection. Cells were cooled to 4°C and stained for NS1 on the surface using the 4NS1 MAb (green). Subsequently, cells were fixed and permeabilized and stained with chimeric human 17NS1 MAb (red) to confirm total levels of NS1. Nuclei were counterstained with TO-PRO-3. The data are representative of two independent experiments. (D) Flow cytometric analysis. BHK21 cells were infected with wild-type or mutant WNV as detailed above. Staining of live intact cells at 4°C assessed the surface levels of wild-type and variant NS1s. Total NS1 and WNV E were determined after fixation, cell permeabilization, and indirect immunofluorescence. Samples were processed by flow cytometry, and data are representative of at least two independent experiments. The *y* axis indicates the number of cells, and the *x* axis shows relative WNV NS1 or E protein level. Shaded histograms are isotype controls.

To evaluate this, we engineered a series of DENV and WNV NS1 chimeras and expressed them ectopically in a double subgenomic SINV. We defined a determinant immediately C-terminal to the signal sequence cleavage position that was responsible for differential cellular targeting. Sequence alignment and site-specific mutagenesis established a short peptide motif centered at amino acid 10 as critical for directing surface targeting and secretion of WNV NS1. Introduction of the corresponding two amino acids (NK or RQ) in this region into WNV or DENV NS1 reciprocally modulated NS1 expression levels on the plasma membrane and secretion in BHK21 cells. When experiments were repeated in C6/36 insect cells, wild-type WNV NS1 secretion was not observed at baseline, consistent with earlier reports with other flaviviruses in these cells (26, 46). However, introduction of the two DENV amino acids (RQ10NK) in this region resulted in accumulation of WNV NS1 in the supernatant (S. Youn and M. S. Diamond, unpublished results); these data agree with a recent report showing low- to even high-level secretion of DENV NS1 in insect cells (42).

When the mutant RQ10NK was engineered into an infectious cDNA clone of WNV, a similar pattern was observed although the virus exhibited a growth defect. This was initially surprising as accumulation of soluble NS1 in late endosomes was reported to enhance DENV infectivity in hepatocytes (1). The basis for the attenuation of RQ10NK WNV remains uncertain although the defect was intrinsic to NS1 as it was *trans*-complemented with wild-type NS1 that was expressed by

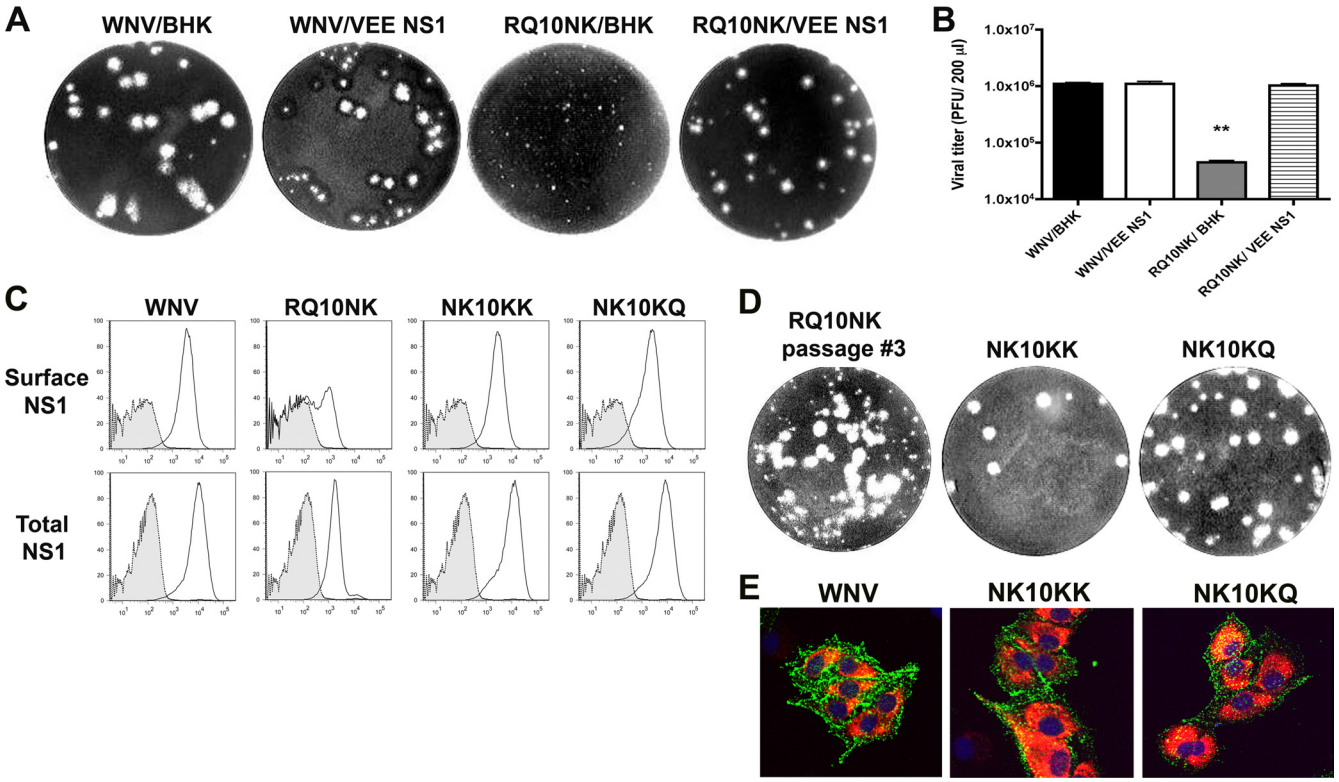

FIG. 11. (A and B) *trans*-Complementation of WNV RQ10NK mutant with VEE-NS1. BHK21 cells (BHK) or BHK21 cells that stably propagate a VEE replicon with a wild-type NS1 transgene (VEE-NS1) were infected with wild-type or RQ10NK WNV. (A) Plaque morphology of wild-type and variant viruses recovered from control BHK or VEE-NS1 cells is shown. (B) Quantitation of secreted virus shows that VEE-NS1 *trans*-complements the replication defect of WNV RQ10NK. Asterisks indicate values that are statistically significant from wild-type WNV infection ($P < 0.0001$). (C to E) Selection and characterization of large-plaque phenotype revertants after three passages of WNV RQ10NK. Based on flow cytometry analysis (C, left panel), the revertant (NK10KK or NK10KQ) was expressed at wild-type levels on the surface of cells. The *y* axis indicates the number of cells, and the *x* axis shows relative NS1 levels. Shaded histograms are isotype controls. Virus titration assays revealed a mixed population of large- and small-plaque phenotypes (D, right panel). The large plaques were picked, expanded, and sequenced. NK10KK and NK10KQ were identified and used for infection of BHK21 cells. The results are representative of two independent experiments. BHK21 cells were infected with recombinant wild-type WNV or revertants (NK10KK and NK10KQ) and harvested at 24 h after infection (E). Cells were cooled to 4°C and stained for NS1 on the surface using the 4NS1 MAb (green). Subsequently, cells were fixed and permeabilized and stained with chimeric human 17NS1 MAb (red) to confirm total levels of NS1. Nuclei were counterstained with TO-PRO-3.

a VEE replicon. Remarkably, two independent revertant viruses of WNV RQ10NK that replicated to wild-type levels of infectivity acquired positive-charge mutations at position 10 (N → K or N → R) and showed wild-type surface expression and secretion patterns. Although further studies are warranted, this finding suggests a link between the effects of NS1 on viral replication and the levels of secreted or cell surface NS1. The precise mechanism by which NS1 acts as a cofactor for viral replication is unclear although a role prior to or at minus-strand synthesis has been postulated (33, 40, 41, 60). We speculate that the attenuated replication phenotype of the RQ10NK variant could be due to accelerated transport through the secretory pathway, with less NS1 in a specific intracellular compartment (e.g., ER) required for cofactor activity. Pulse-chase studies showed a shorter time of residence in the ER of the RQ10NK variant than of the wild-type WNV NS1. Finally, sequence alignment of NS1 from all globally relevant human flaviviruses revealed that all four serotypes of DENV differ from the remainder of viruses within the genus (Fig. 6A) at position 10: DENV strains contain the amino acids N, G, or S, with none containing basic (R or K) residues at this position.

We further explored the mechanism by which the RQ → NK change altered secretion of WNV NS1. Based on computer prediction algorithms, we hypothesized that the RQ10NK mutant might have a downstream signal peptide cleavage site that would increase the secretion efficiency of NS1. However, N-terminal sequencing of secreted RQ10NK or AI5VV NS1 revealed no difference in cleavage site or the bona fide N terminus of the proteins. We speculate that the RQ → NK change alters the relative trafficking rate and destination of WNV NS1 through the secretory pathway by decreasing interactions with uncharacterized host proteins or polar lipids. Indeed, during our pulse-chase analysis, the pool of endo H-sensitive RQ10NK NS1 was noticeably less than that of wild-type WNV NS1. One candidate protein for differential interaction is the ER-resident chaperone calnexin, which was coimmunoprecipitated by JEV NS1 (66).

Our experiments revealed an independent requirement of N-linked glycans for efficient secretion but, surprisingly, not for

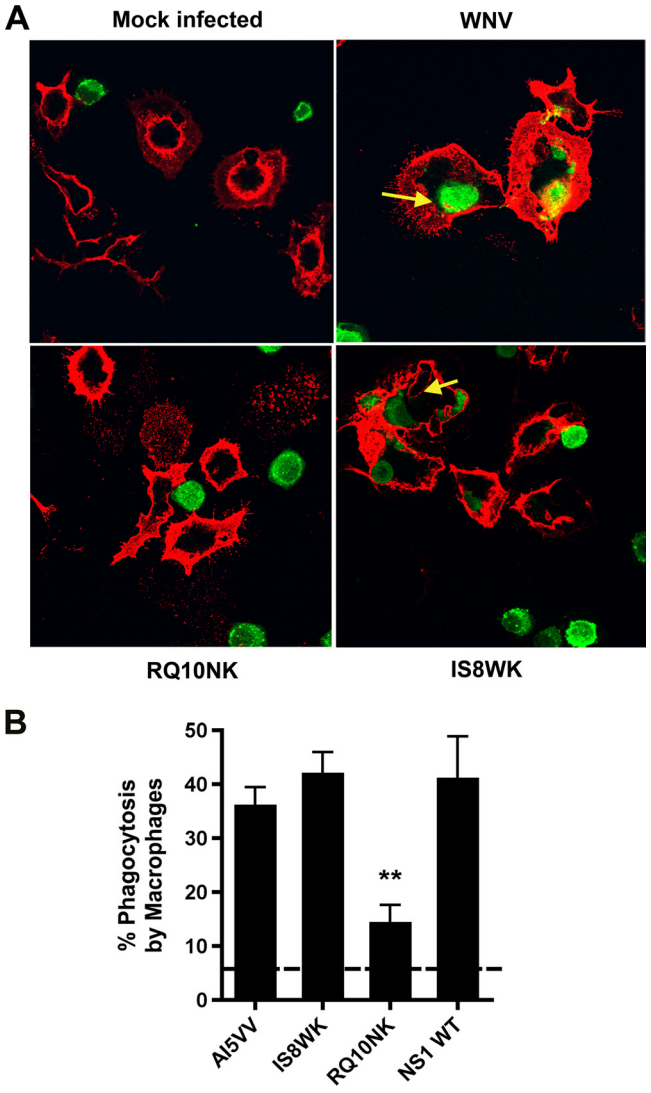

FIG. 12. Anti-NS1 MAb-dependent phagocytosis by peritoneal macrophages. (A) Thioglycolate-elicited peritoneal macrophages were isolated after peritoneal lavage from wild-type C57BL/6 mice and adhered (5×10^5 cells) on poly-D-lysine and laminin-coated coverslips. BHK21 cells were infected with wild-type, RQ10NK, and IS8WK WNV, and 30 h later, cells were labeled with CFSE, fixed, opsonized with 10NS1 or an isotype control (data not shown), and incubated with peritoneal macrophages for 2 h at 37°C. Note, a higher MOI was used for the RQ10NK variant to achieve equivalent infection as judged by intracellular E and NS1 staining, and virus titration was performed by plaque assay (Fig. 8; also data not shown) (see text). After cells were washed, they were fixed, stained with APC-conjugated anti-mouse CD11b, and imaged by confocal microscopy. The yellow arrows indicate CFSE-labeled infected BHK21 target cells engulfed by macrophages. (B) Quantitation of the percentage of phagocytosed WNV-infected target cells by peritoneal macrophages after opsonization with 10NS1 MAb. Ten to 15 random fields (~200 cells) were counted (magnification, ×63) per variant for each experiment. The difference in numbers of phagocytosed cells between the wild-type and RQ10NK WNV was statistically significant ($P < 0.05$) and reflects pooled data from three independent experiments. The dashed lines indicate the basal phagocytosis rate by macrophages of uninfected cells.

plasma membrane expression or distribution of NS1. While previous studies with YFV, JEV, and DENV NS1 had established that ablation of N-linked glycans impairs secretion (46, 48, 52), surface expression of these mutants was not examined. Our results are consistent, however, with a study showing that tunicamycin treatment, which abrogates addition of N-linked glycans, did not alter the plasma membrane expression of DENV NS1 (65). N-linked glycosylation may facilitate directly or indirectly the generation of NS1 hexamers, a form of NS1 that is preferentially secreted (16, 26). In contrast, surface NS1 on infected cells, which is displayed as a dimer (64, 65), lacks a requirement for addition of N-linked glycans. This is most apparent in our studies with the glycosylation null mutant of WNV NS1.

The pulse-chase studies also suggested that secreted NS1 accumulates in cell supernatants with carbohydrate side chains that are partially resistant to endo H treatment. This finding of partial sensitivity to endo H of secreted WNV NS1 is consistent with previous observations for DENV (50), YFV (18), and JEV (46). Interestingly, inhibition of conversion to N-linked high-mannose glycans to hybrid/complex oligosaccharides with deoxymannojirimycin did not markedly alter WNV NS1 secretion. These data differ from observations with DENV NS1 (26, 66) although in those studies the glycosylation inhibitors were included for 20 h, which is sufficient time to reduce DENV replication (14, 61), a phenomena that could confound interpretation of rates of NS1 production and secretion. The biosynthetic labeling experiments also showed that at 6 h postchase, the intracellular forms of the RQ10NK variant were almost completely endo H sensitive, in contrast to wild-type WNV or other variants. We interpret this to mean that the transit time of NS1 from the endoplasmic reticulum is rather slow, possibly due to a specific retention mechanism or a requirement for chaperone-dependent folding (66). Once NS1 reaches the Golgi compartment, however, it likely transits rapidly to the surface or is secreted. For mutants like RQ10NK, where there is little surface compared to secreted NS1, the endo H-resistant fraction accumulates in the supernatant (Fig. 8A). In contrast, in cells infected with wild-type virus, significant amounts of endo H-resistant NS1 are displayed on the plasma membrane. Although further studies are warranted, we speculate that the endo H-resistant form of NS1 in lysates of wild-type WNV-infected cells largely reflects the pool that is displayed on the cell surface.

Combining our results with those published by others, we propose a model for the relationship between cell surface expression and secretion of flavivirus NS1 (Fig. 13). The signal sequence of NS1 (C terminus of E) targets the nascent viral polypeptide to the lumen of ER. Upon completion of protein synthesis, NS1 monomers associate to become dimers in a manner that does not require N-linked glycosylation. WNV NS1 (which contains R10Q11) is retained to a greater extent in the ER in an endo H-sensitive form than DENV NS1 (which contains N10K11), perhaps by association with a resident ER protein. Transport to the Golgi compartment facilitates carbohydrate modification to a partially endo H-resistant hybrid/complex N-linked glycan. We propose that the peptide motif centered at position 10 of WNV NS1 facilitates an interaction with a membrane-associated moiety that promotes retention on the plasma membrane. In contrast, the DENV peptide

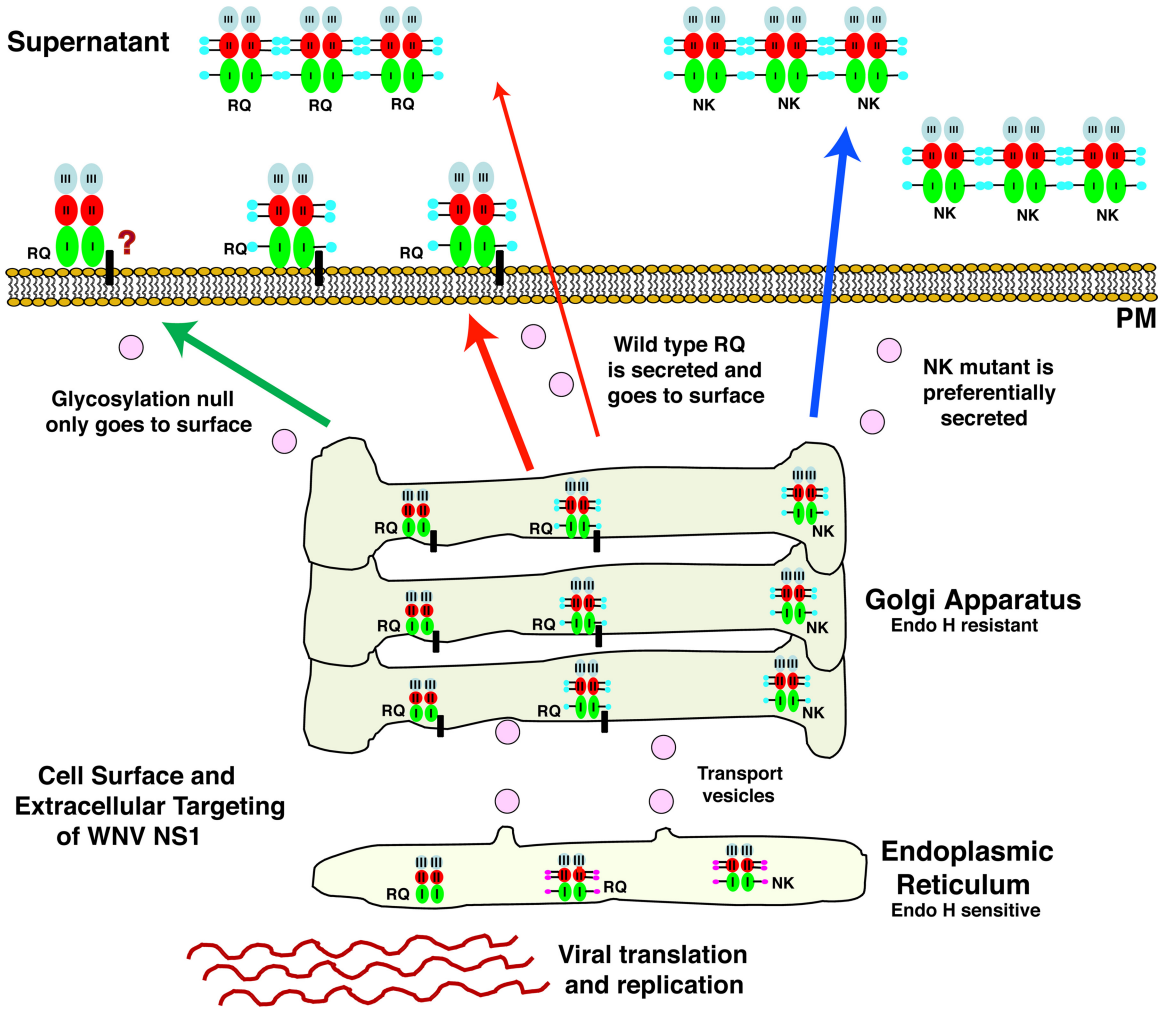

FIG. 13. Model of regulation of cellular compartmentalization of flavivirus NS1. Flavivirus replication occurs at the cytoplasmic face of the rough ER. Because of its signal sequence (which corresponds to the C-terminal region of the E gene), NS1 is synthesized and extruded into the lumen of the ER. Here, depending on the N-terminal region sequence (e.g., RQ or NK), NS1 may associate differentially with an as yet undefined ER retention protein. Retention of NS1 (endo H sensitive) in the ER sustains flavivirus replication possibly by associating with an ER transmembrane protein that has a key functional domain on the cytoplasmic face. NS1 is transported to the Golgi network with concomitant modification of N-linked glycans to hybrid/complex oligosaccharides (endo H resistant). Depending on the specific sequence in the N-terminal region and presence of N-linked glycans, different patterns of targeting are observed. For NS1 that lack all N-linked glycans (e.g., NS1 CHO null), cell surface expression exclusively ensues. Prior studies have suggested that cell surface NS1 is present as a homodimer (64, 65). For NS1 with DENV-like sequences in the N-terminal region (e.g., NK10-11), protein is preferentially secreted with lower levels targeted to the cell surface. For NS1 with WNV-like sequences (e.g., RQ10-11), protein is preferentially displayed on the cell surface with lower levels of secretion. This may be due to association with an uncharacterized resident membrane protein or polar lipid (indicated by a question mark). N-linked glycosylation may facilitate directly or indirectly generation of higher-order NS1 hexamers, which are the form of NS1 that is preferentially secreted (16, 26). However, while modification of N-linked glycans to the endo H-resistant form occurs with trafficking through the Golgi network, studies with the alpha-mannosidase I inhibitor deoxymannojirimycin show that it is not required for secretion.

motif at this corresponding position weakly associates with this moiety, thus facilitating secretion into the cell supernatant. Based on studies with null mutants and inhibitors, the N-linked glycosylation requirements for surface expression and secretion are as follows: (i) surface NS1, which is a dimer, does not require N-linked glycosylation; and (ii) secreted NS1, which is a hexamer, requires N-linked glycans, possibly for oligomeric formation or stabilization. Although some of the N-linked glycans on NS1 are modified in the Golgi network, there is no absolute requirement of this for secretion, as indicated by studies with deoxymannojirimycin. Finally, higher levels of surface NS1 are associated reciprocally with decreased levels of secretion.

What is the impact of altering the cellular targeting of NS1? By changing the surface levels through site-specific substitutions in the N-terminal region of NS1, antibody recognition and immune clearance of WNV-infected cells by activated macrophages are altered. Recombinant WNVs expressing the RQ10NK mutation were more resistant to antibody-induced phagocytosis. Different flaviviruses may modulate their intracellular, surface, and secreted NS1 levels to balance particular proviral functions (cofactor for viral replicase and complement

antagonist) with antiviral responses by the host (antibody recognition and clearance of infected cells).

ACKNOWLEDGMENTS

We thank W. Klimstra and D. Lenschow for the SINV expression constructs, I. Frolov for the VEE replicon, W. Beatty for expertise with the confocal microscopy, C. Nelson for help with the N-terminal protein sequencing and protein alignments, M. Edeling for critical comments on the manuscript, and P. Avirutnan for anti-DENV NS1 MAbs.

This work was supported by the Pediatric Dengue Vaccine Initiative and Midwest Regional Centers of Excellence for Biodefense and Emerging Infectious Disease Research (U54-AI057160).

REFERENCES

1. **Alcon-LePoder, S., M. T. Drouet, P. Roux, M. P. Frenkiel, M. Arborio, A. M. Durand-Schneider, M. Maurice, I. Le Blanc, J. Gruenberg, and M. Flamand.** 2005. The secreted form of dengue virus nonstructural protein NS1 is endocytosed by hepatocytes and accumulates in late endosomes: implications for viral infectivity. J. Virol. **79:**11403–11411.
2. **Alcon-LePoder, S., P. Sivard, M. T. Drouet, A. Talarmin, C. Rice, and M. Flamand.** 2006. Secretion of flaviviral non-structural protein NS1: from diagnosis to pathogenesis. Novartis Found. Symp. **277:**233–247; discussion 247–253.
3. **Avirutnan, P., A. Fuchs, R. E. Hauhart, P. Somnuke, S. Youn, M. S. Diamond, and J. P. Atkinson.** 2010. Antagonism of the complement component C4 by flavivirus non-structural protein NS1. J. Exp. Med. **207:**793–806.
4. **Avirutnan, P., N. Punyadee, S. Noisakran, C. Komoltri, S. Thiemmeca, K. Auethavornanan, A. Jairungsri, R. Kanlaya, N. Tangthawornchaikul, C. Puttikhunt, S. N. Pattanakitsakul, P. T. Yenchitsomanus, J. Mongkolsapaya, W. Kasinrerk, N. Sittisombut, M. Husmann, M. Blettner, S. Vasanawathana, S. Bhakdi, and P. Malasit.** 2006. Vascular leakage in severe dengue virus infections: a potential role for the nonstructural viral protein NS1 and complement. J. Infect. Dis. **193:**1078–1088.
5. **Avirutnan, P., L. Zhang, N. Punyadee, A. Manuyakorn, C. Puttikhunt, W. Kasinrerk, P. Malasit, J. P. Atkinson, and M. S. Diamond.** 2007. Secreted NS1 of dengue virus attaches to the surface of cells via interactions with heparan sulfate and chondroitin sulfate E. PLoS Pathog. **3:**e183.
6. **Baeuerle, P. A., and W. B. Huttner.** 1986. Chlorate—a potent inhibitor of protein sulfation in intact cells. Biochem. Biophys. Res. Commun. **141:**870–877.
7. **Beasley, D. W., M. C. Whiteman, S. Zhang, C. Y. Huang, B. S. Schneider, D. R. Smith, G. D. Gromowski, S. Higgs, R. M. Kinney, and A. D. Barrett.** 2005. Envelope protein glycosylation status influences mouse neuroinvasion phenotype of genetic lineage 1 West Nile virus strains. J. Virol. **79:**8339–8347.
8. **Blitvich, B. J., D. Scanlon, B. J. Shiell, J. S. Mackenzie, and R. A. Hall.** 1999. Identification and analysis of truncated and elongated species of the flavivirus NS1 protein. Virus Res. **60:**67–79.
9. **Busch, M. P., D. J. Wright, B. Custer, L. H. Tobler, S. L. Stramer, S. H. Kleinman, H. E. Prince, C. Bianco, G. Foster, L. R. Petersen, G. Nemo, and S. A. Glynn.** 2006. West Nile virus infections projected from blood donor screening data, United States, 2003. Emerg. Infect. Dis. **12:**395–402.
10. **Chung, K. M., and M. S. Diamond.** 2008. Defining the levels of secreted non-structural protein NS1 after West Nile virus infection in cell culture and mice. J. Med. Virol. **80:**547–556.
11. **Chung, K. M., M. K. Liszewski, G. Nybakken, A. E. Davis, R. R. Townsend, D. H. Fremont, J. P. Atkinson, and M. S. Diamond.** 2006. West Nile virus non-structural protein NS1 inhibits complement activation by binding the regulatory protein factor H. Proc. Natl. Acad. Sci. U. S. A. **103:**19111–19116.
12. **Chung, K. M., G. E. Nybakken, B. S. Thompson, M. J. Engle, A. Marri, D. H. Fremont, and M. S. Diamond.** 2006. Antibodies against West Nile virus nonstructural protein NS1 prevent lethal infection through Fc gamma receptor-dependent and -independent mechanisms. J. Virol. **80:**1340–1351.
13. **Chung, K. M., B. S. Thompson, D. H. Fremont, and M. S. Diamond.** 2007. Antibody recognition of cell surface-associated NS1 triggers Fc-γ receptor-mediated phagocytosis and clearance of West Nile virus-infected cells. J. Virol. **81:**9551–9555.
14. **Courageot, M. P., M. P. Frenkiel, C. D. Dos Santos, V. Deubel, and P. Despres.** 2000. α-Glucosidase inhibitors reduce dengue virus production by affecting the initial steps of virion morphogenesis in the endoplasmic reticulum. J. Virol. **74:**564–572.
15. **Crabtree, M. B., R. M. Kinney, and B. R. Miller.** 2005. Deglycosylation of the NS1 protein of dengue 2 virus, strain 16681: construction and characterization of mutant viruses. Arch. Virol. **150:**771–786.
16. **Crooks, A. J., J. M. Lee, L. M. Easterbrook, A. V. Timofeev, and J. R. Stephenson.** 1994. The NS1 protein of tick-borne encephalitis virus forms multimeric species upon secretion from the host cell. J. Gen. Virol. **75:**3453–3460.
17. **Despres, P., J. Dietrich, M. Girard, and M. Bouloy.** 1991. Recombinant baculoviruses expressing yellow fever virus E and NS1 proteins elicit protective immunity in mice. J. Gen. Virol. **72:**2811–2816.
18. **Despres, P., M. Girard, and M. Bouloy.** 1991. Characterization of yellow fever virus proteins E and NS1 expressed in Vero and Spodoptera frugiperda cells. J. Gen. Virol. **72:**1331–1342.
19. **Diamond, M. S., B. Shrestha, A. Marri, D. Mahan, and M. Engle.** 2003. B cells and antibody play critical roles in the immediate defense of disseminated infection by West Nile encephalitis virus. J. Virol. **77:**2578–2586.
20. **Ebel, G. D., A. P. Dupuis III, K. Ngo, D. Nicholas, E. Kauffman, S. A. Jones, D. Young, J. Maffei, P. Y. Shi, K. Bernard, and L. Kramer.** 2001. Partial genetic characterization of West Nile virus strains, New York State, 2000. Emerg. Infect. Dis. **7:**650–653.
21. **Falconar, A. K.** 1997. The dengue virus nonstructural-1 protein (NS1) generates antibodies to common epitopes on human blood clotting, integrin/adhesin proteins and binds to human endothelial cells: potential implications in haemorrhagic fever pathogenesis. Arch. Virol. **142:**897–916.
22. **Falgout, B., M. Bray, J. J. Schlesinger, and C. J. Lai.** 1990. Immunization of mice with recombinant vaccinia virus expressing authentic dengue virus nonstructural protein NS1 protects against lethal dengue virus encephalitis. J. Virol. **64:**4356–4363.
23. **Falgout, B., R. Chanock, and C. J. Lai.** 1989. Proper processing of dengue virus nonstructural glycoprotein NS1 requires the N-terminal hydrophobic signal sequence and the downstream nonstructural protein NS2a. J. Virol. **63:**1852–1860.
24. **Fan, W. F., and P. W. Mason.** 1990. Membrane association and secretion of the Japanese encephalitis virus NS1 protein from cells expressing NS1 cDNA. Virology **177:**470–476.
25. **Firth, A. E., and J. F. Atkins.** 2009. A conserved predicted pseudoknot in the NS2A-encoding sequence of West Nile and Japanese encephalitis flaviviruses suggests NS1′ may derive from ribosomal frameshifting. Virol. J. **6:**14.
26. **Flamand, M., F. Megret, M. Mathieu, J. Lepault, F. A. Rey, and V. Deubel.** 1999. Dengue virus type 1 nonstructural glycoprotein NS1 is secreted from mammalian cells as a soluble hexamer in a glycosylation-dependent fashion. J. Virol. **73:**6104–6110.
27. **Gould, E. A., A. Buckley, A. D. Barrett, and N. Cammack.** 1986. Neutralizing (54K) and non-neutralizing (54K and 48K) monoclonal antibodies against structural and non-structural yellow fever virus proteins confer immunity in mice. J. Gen. Virol. **67:**591–595.
28. **Halstead, S. B.** 1970. Observations related to pathogensis of dengue hemorrhagic fever. VI. Hypotheses and discussion. Yale J. Biol. Med. **42:**350–362.
29. **Henchal, E. A., L. S. Henchal, and J. J. Schlesinger.** 1988. Synergistic interactions of anti-NS1 monoclonal antibodies protect passively immunized mice from lethal challenge with dengue 2 virus. J. Gen. Virol. **69:**2101–2107.
30. **Jacobs, M. G., P. J. Robinson, C. Bletchly, J. M. Mackenzie, and P. R. Young.** 2000. Dengue virus nonstructural protein 1 is expressed in a glycosyl-phosphatidylinositol-linked form that is capable of signal transduction. FASEB J. **14:**1603–1610.
31. **Jacobs, S. C., J. R. Stephenson, and G. W. Wilkinson.** 1992. High-level expression of the tick-borne encephalitis virus NS1 protein by using an adenovirus-based vector: protection elicited in a murine model. J. Virol. **66:**2086–2095.
32. **Jacobs, S. C., J. R. Stephenson, and G. W. Wilkinson.** 1994. Protection elicited by a replication-defective adenovirus vector expressing the tick-borne encephalitis virus non-structural glycoprotein NS1. J. Gen. Virol. **75:**2399–2402.
33. **Khromykh, A. A., P. L. Sedlak, and E. G. Westaway.** 2000. *cis*- and *trans*-Acting elements in flavivirus RNA replication. J. Virol. **74:**3253–3263.
34. **Khromykh, A. A., P. L. Sedlak, and E. G. Westaway.** 1999. *trans*-Complementation analysis of the flavivirus Kunjin ns5 gene reveals an essential role for translation of its N-terminal half in RNA replication. J. Virol. **73:**9247–9255.
35. **Kinney, R. M., S. Butrapet, G. J. Chang, K. R. Tsuchiya, J. T. Roehrig, N. Bhamarapravati, and D. J. Gubler.** 1997. Construction of infectious cDNA clones for dengue 2 virus: strain 16681 and its attenuated vaccine derivative, strain PDK-53. Virology **230:**300–308.
36. **Krishna, V. D., M. Rangappa, and V. Satchidanandam.** 2009. Virus-specific cytolytic antibodies to nonstructural protein 1 of Japanese encephalitis virus effect reduction of virus output from infected cells. J. Virol. **83:**4766–4777.
37. **Libraty, D. H., P. R. Young, D. Pickering, T. P. Endy, S. Kalayanarooj, S. Green, D. W. Vaughn, A. Nisalak, F. A. Ennis, and A. L. Rothman.** 2002. High circulating levels of the dengue virus nonstructural protein NS1 early in dengue illness correlate with the development of dengue hemorrhagic fever. J. Infect. Dis. **186:**1165–1168.
38. **Lin, C. F., H. Y. Lei, A. L. Shiau, C. C. Liu, H. S. Liu, T. M. Yeh, S. H. Chen, and Y. S. Lin.** 2003. Antibodies from dengue patient sera cross-react with endothelial cells and induce damage. J. Med. Virol. **69:**82–90.
39. **Lindenbach, B. D., and C. M. Rice.** 2001. *Flaviviridae*: the viruses and their replication, p. 991–1041. *In* D. M. Knipe, P. M. Howley, D. E. Griffin, R. A. Lamb, M. A. Martin, B. Roizman, and S. E. Straus (ed.), Fields virology, vol. 1, 4th ed. Lippincott Williams & Wilkins, Philadelphia, PA.
40. **Lindenbach, B. D., and C. M. Rice.** 1999. Genetic interaction of flavivirus

nonstructural proteins NS1 and NS4A as a determinant of replicase function. J. Virol. **73:**4611–4621.
41. **Lindenbach, B. D., and C. M. Rice.** 1997. trans-Complementation of yellow fever virus NS1 reveals a role in early RNA replication. J. Virol. **71:**9608–9617.
42. **Ludert, J. E., C. Mosso, I. Ceballos-Olvera, and R. M. del Angel.** 2008. Use of a commercial enzyme immunoassay to monitor dengue virus replication in cultured cells. Virol. J. **5:**51.
43. **Macdonald, J., J. Tonry, R. A. Hall, B. Williams, G. Palacios, M. S. Ashok, O. Jabado, D. Clark, R. B. Tesh, T. Briese, and W. I. Lipkin.** 2005. NS1 protein secretion during the acute phase of West Nile virus infection. J. Virol. **79:**13924–13933.
44. **Mackenzie, J. M., M. K. Jones, and P. R. Young.** 1996. Immunolocalization of the dengue virus nonstructural glycoprotein NS1 suggests a role in viral RNA replication. Virology **220:**232–240.
45. **Mackenzie, J. S., D. J. Gubler, and L. R. Petersen.** 2004. Emerging flaviviruses: the spread and resurgence of Japanese encephalitis, West Nile and dengue viruses. Nat. Med. **10:**S98–109.
46. **Mason, P. W.** 1989. Maturation of Japanese encephalitis virus glycoproteins produced by infected mammalian and mosquito cells. Virology **169:**354–364.
47. **Melian, E. B., E. Hinzman, T. Nagasaki, A. E. Firth, N. M. Wills, A. S. Nouwens, B. J. Blitvich, J. Leung, A. Funk, J. F. Atkins, R. Hall, and A. A. Khromykh.** 2010. NS1′ of flaviviruses in the Japanese encephalitis virus serogroup is a product of ribosomal frameshifting and plays a role in viral neuroinvasiveness. J. Virol. **84:**1641–1647.
48. **Muylaert, I. R., T. J. Chambers, R. Galler, and C. M. Rice.** 1996. Mutagenesis of the N-linked glycosylation sites of the yellow fever virus NS1 protein: effects on virus replication and mouse neurovirulence. Virology **222:**159–168.
49. **Noisakran, S., T. Dechtawewat, P. Avirutnan, T. Kinoshita, U. Siripanyaphinyo, C. Puttikhunt, W. Kasinrerk, P. Malasit, and N. Sittisombut.** 2008. Association of dengue virus NS1 protein with lipid rafts. J. Gen. Virol. **89:**2492–2500.
50. **Noisakran, S., T. Dechtawewat, P. Rinkaewkan, C. Puttikhunt, A. Kanjanahaluethai, W. Kasinrerk, N. Sittisombut, and P. Malasit.** 2007. Characterization of dengue virus NS1 stably expressed in 293T cell lines. J. Virol. Methods **142:**67–80.
51. **Oliphant, T., M. Engle, G. Nybakken, C. Doane, S. Johnson, L. Huang, S. Gorlatov, E. Mehlhop, A. Marri, K. M. Chung, G. D. Ebel, L. D. Kramer, D. H. Fremont, and M. S. Diamond.** 2005. Development of a humanized monoclonal antibody with therapeutic potential against West Nile virus. Nat. Med. **11:**522–530.
52. **Pryor, M. J., and P. J. Wright.** 1994. Glycosylation mutants of dengue virus NS1 protein. J. Gen. Virol. **75:**1183–1187.
53. **Pugachev, K. V., P. W. Mason, R. E. Shope, and T. K. Frey.** 1995. Double-subgenomic Sindbis virus recombinants expressing immunogenic proteins of Japanese encephalitis virus induce significant protection in mice against lethal JEV infection. Virology **212:**587–594.
54. Reference deleted.
55. **Ryman, K. D., C. L. Gardner, C. W. Burke, K. C. Meier, J. M. Thompson, and W. B. Klimstra.** 2007. Heparan sulfate binding can contribute to the neurovirulence of neuroadapted and nonneuroadapted Sindbis viruses. J. Virol. **81:**3563–3573.
56. **Schlesinger, J. J., M. W. Brandriss, C. B. Cropp, and T. P. Monath.** 1986. Protection against yellow fever in monkeys by immunization with yellow fever virus nonstructural protein NS1. J. Virol. **60:**1153–1155.
57. **Schlesinger, J. J., M. W. Brandriss, and E. E. Walsh.** 1985. Protection against 17D yellow fever encephalitis in mice by passive transfer of monoclonal antibodies to the nonstructural glycoprotein gp48 and by active immunization with gp48. J. Immunol. **135:**2805–2809.
58. **Schlesinger, J. J., M. Foltzer, and S. Chapman.** 1993. The Fc portion of antibody to yellow fever virus NS1 is a determinant of protection against YF encephalitis in mice. Virology **192:**132–141.
59. **Sejvar, J. J., M. B. Haddad, B. C. Tierney, G. L. Campbell, A. A. Marfin, J. A. Van Gerpen, A. Fleischauer, A. A. Leis, D. S. Stokic, and L. R. Petersen.** 2003. Neurologic manifestations and outcome of West Nile virus infection. JAMA **290:**511–515.
60. **Westaway, E. G., J. M. Mackenzie, M. T. Kenney, M. K. Jones, and A. A. Khromykh.** 1997. Ultrastructure of Kunjin virus-infected cells: colocalization of NS1 and NS3 with double-stranded RNA, and of NS2B with NS3, in virus-induced membrane structures. J. Virol. **71:**6650–6661.
61. **Whitby, K., T. C. Pierson, B. Geiss, K. Lane, M. Engle, Y. Zhou, R. W. Doms, and M. S. Diamond.** 2005. Castanospermine, a potent inhibitor of dengue virus infection in vitro and in vivo. J. Virol. **79:**8698–8706.
62. **Whiteman, M. C., L. Li, J. A. Wicker, R. M. Kinney, C. Huang, D. W. Beasley, K. M. Chung, M. S. Diamond, T. Solomon, and A. D. Barrett.** 2010. Development and characterization of non-glycosylated E and NS1 mutant viruses as a potential candidate vaccine for West Nile virus. Vaccine **28:**1075–1083.
63. **Wilson, J. R., P. F. de Sessions, M. A. Leon, and F. Scholle.** 2008. West Nile virus nonstructural protein 1 inhibits TLR3 signal transduction. J. Virol. **82:**8262–8271.
64. **Winkler, G., S. E. Maxwell, C. Ruemmler, and V. Stollar.** 1989. Newly synthesized dengue-2 virus nonstructural protein NS1 is a soluble protein but becomes partially hydrophobic and membrane-associated after dimerization. Virology **171:**302–305.
65. **Winkler, G., V. B. Randolph, G. R. Cleaves, T. E. Ryan, and V. Stollar.** 1988. Evidence that the mature form of the flavivirus nonstructural protein NS1 is a dimer. Virology **162:**187–196.
66. **Wu, S. F., C. J. Lee, C. L. Liao, R. A. Dwek, N. Zitzmann, and Y. L. Lin.** 2002. Antiviral effects of an iminosugar derivative on flavivirus infections. J. Virol. **76:**3596–3604.
67. **Yount, B., M. R. Denison, S. R. Weiss, and R. S. Baric.** 2002. Systematic assembly of a full-length infectious cDNA of mouse hepatitis virus strain A59. J. Virol. **76:**11065–11078.